Eidgenössische Technische Hochschule Zürich
Swiss Federal Institute of Technology Zurich

Institute for Atmospheric and Climate Science

Master Thesis

How to Distribute New Solar Systems in Europe to Reduce Power Generation Variability

Department Environmental Systems Science / Earth Sciences, ETH Zürich
Institute for Atmospheric and Climate Science

Supervisors:
Dr. Jan Wohland, Institute for Environmental Decisions, ETH Zürich
Dr. Doris Sylvia Folini, Institute for Atmospheric and Climate Science, ETH Zürich
Dr. Stefan Pfenninger, Institute for Environmental Decisions, ETH Zürich
Prof. Dr. Martin Wild, Institute for Atmospheric and Climate Science, ETH Zürich

Submitted by
Dirk Mühlemann
13-732-037
Uster, 01/05/2021

Abstract

To reduce greenhouse gas emissions and combat climate change, the electrical power production sector is facing a fundamental transition from conventional fossil to renewable technologies. The transition has already started, which can be seen by the great effort and ambitious targets of many nations around the globe. Installed power production capacities of solar photovoltaics (PV) are increasing every year and are already capable of producing around 5.5% of the Europeans electricity demand. Since PV power output depends on weather and climate, it exhibits a highly variable production pattern. This variability challenges the electricity grids because the stability of the grids depends on balanced supply and demand. Further massive deployment of PV systems could lead to an increase of the variability and therefore add to this challenge. Different studies suggest strategies to reduce the PV power output variability on rather short (minutes to hours) or long (seasonal) timescales. However, weather regimes lasting several days influence the PV power output across Europe as well, and knowledge of its impact on multiday PV power output variability is still limited.

Within this thesis, we identify spatial distributions of newly installed PV systems that minimize the multiday power output variability in Europe. To quantify the variability, we perform empirical orthogonal function (EOF) analyses of geopotential height at 500hPa, which reflects weather regimes and therefore has an indirect effect on the PV power output. The geopotential height field is taken from the ERA5 reanalysis dataset which covers the time period from 1979 to present. The resulting subspace spanned by the leading 14 EOFs (explains ~90% if the variance) of our analysis is grouped in seven different weather regimes with the k-mean clustering techniques. To assess the PV power output variability the resulted regimes are linked to country specific PV capacity factors. We use hourly PV capacity factors provided by the simulation of renewable.ninja from 1985-2019. Connecting the regimes with the PV capacity factors leads to an overview of under- and overproduction (relative to the mean) per country and weather regime. Current and planned (NECPs 2030) installed capacity of PV systems in Europe is used together with our findings to assess the current and future multiday PV power output variability in Europe. Furthermore, an optimal (linear least square fit) distribution of additional PV systems is calculated which minimize the multiday variability.

The mean variability, which is the average change of PV power production from one weather regime to another, currently (2019) amounts to 0.9 GW. Whereas the current maximum variability, which is the change of PV power production from the weather regime with the highest PV production to the one with the lowest production, amounts to 3.0 GW. We estimate that with the planed installed PV capacity distribution of the NECPs this is expected to triple by 2030 to 2.7GW and 8.5GW, respectively. Estimates for the year 2050 emphasise that the mean variability could increase from 6.4 GW up to 63.2 GW (depending on the scenario) and the maximum variability could even increase from 20.1 GW to 198.6 GW. We could show that a reduction of the variability for different scenarios of future installed PV capacity distribution is possible. Our method was able to reduce the mean variability up to 44.4 % and the maximum variability up

to 38.8 %. The reduction could be achieved by mainly placing the new installed PV capacity to South-eastern and to North-western Europe.

Contents

1. Introduction 6
2. Data & Methods 9
2.1 Data 9
2.1.1 ERA5 9
2.1.2 Renewables.ninja and the Global Solar Energy Estimator (GSEE) 9
2.1.3 Installed PV capacities 13
2.1.4 Electricity consumption data 13
2.2 Method 14
2.2.1 ERA5 data pre-processing 15
2.2.2 Weather regime classification 16
2.2.3 Capacity factors 16
2.2.4 Variability reduction with optimal IC distribution 17
2.2.5 Scenarios 18
3. Results 21
3.1 Weather regimes and their linked capacity factor anomalies 21
3.1.1 Weather regime 0 / NOA+ 26
3.1.2 Weather regime 1 - European trough 26
3.1.3 Weather regime 2 – NOA- 27
3.1.4 Weather regime 3 - Atlantic ridge 27
3.1.5 Weather regime 4 - Atlantic trough 27
3.1.6 Weather regime 5 - European blocking 28
3.1.7 Weather regime 6 - Scandinavian blocking 28
3.1.8 No regime 28
3.2 Installed capacity distributions and their variability 30
3.2.1 Scenario 1 (S1) – PV power production and installed capacities from NECP 2030 31
3.2.2 Scenario 2 (S2) – PV IC in 2050 34

3.2.3 Scenario 3 (S3) – Cost minimization..... 36

3.2.4 Scenario 4 (S4) –Coverage of country specific electricity consumption with PV systems 37

3.3 Notes..... 41

3.4 Scenarios for IC distribution ..... **Fehler! Textmarke nicht definiert.**

3.4.1 S1..... **Fehler! Textmarke nicht definiert.**

4. Discussion and conclusion 42

5. Appendix 49

7. References 51

1. Introduction

Many governments undertake ambitious climate mitigation efforts to reduce the adverse effect of global warming and thereby try to meet the 1.5°C goal from the Paris agreement (Hulme, 2016). To achieve this goal a transition from conventional fossil to renewable energy technologies is substantial. Solar power generating photovoltaic (PV) systems, as one of the major renewable technologies, has seen a tremendous growth in recent years. According to the PV status report (2019) by the European commission, there was a global installed capacity of 520GW by the end of 2018. By the end of 2019, the installed capacity is expected to reach 650GW, which allows the PV systems to produce roughly 4% of the global electricity demand. Europe's share of installed PV capacity at the end of 2018 was about 117GW, which allowed to produce 5.5% of Europeans electricity demand. Furthermore, recent scenarios for the necessary installed PV capacity if the world is to reach 100 % renewable electricity production in 2050, suggest that the PV installed capacity must rise to more than 4TW by 2025 and 21.9TW by 2050. For Europe this would imply an PV installed capacity of 630GW by 2025 and 1.94TW by 2050 (Jäger-Waldau, 2019).

→ plan from NCEP for 2030

-→ other studies i.e. IRENA → 0.8TW

PV power output depends on weather and climate and therefore challenges the current power grid by variable power input (Graabak & Korpås, 2016; Stram, 2016). → Drücke 2020 James 2007

Within minutes, the power production from a PV system can vary by as much as 80% due to passing broken cloud cover (Mills & Wiser, 2010). There is also a diurnal cycle with highest power production during the day and no production during night. By analysing multiday fluctuation, a relation between long lasting weather regimes and PV power production can be observed. During one weather regime the PV production pattern varies substantially to the next weather regime (Grams et al., 2017). Furthermore, variability in the PV power production is caused by the seasonal cycle (Heide et al., 2010). The efficiency of a PV panel is mainly dominated by the available surface solar radiation and the panel temperature (Huld et al., 2010). Since the seasonal cycle affects both, a direct effect can be observed. Even decadal to multidecadal analyses suggest that global warming and solar brightening/dimming influences the PV power output. Solar brightening/dimming is often caused by air pollution patterns, which influences the available surface solar radiation and therefore affects the PV power output. Global warming leads to an increase of panel temperatures and reduces the efficiency of the panels (Sweerts et al., 2019; Wild et al., 2015).

A stable power grid depends on balanced electrical supply and demand (Stram, 2016).

Frequency example → what happens if not!?? → Hirth and Ziegenhagen 2015, Garnier and Madlener 2015

➔ Energy balancing Kiviluoma 2012

Short time scale variability due to passing broken cloud cover can affect one PV system substantially. But wider geographical distribution of multiple interconnected PV systems can significantly smooth this short time PV power output variability (Delucchi & Jacobson, 2011; Graabak & Korpås, 2016). Co-deployment of renewable energy system (water, wind and solar) can counteract the variable power output caused by diurnal and seasonal cycles. The basis for these approaches is the different diurnal and seasonal production pattern of water, wind and solar power plants. For example, wind power output exhibits highest production rates during winter whereas solar power production is highest in summer. Co-deployment of wind and solar can therefore reduce the seasonal power production variability. Other combination are possible as well (Graabak & Korpås, 2016; Heide et al., 2010; Santos-Alamillos et al., 2015). To summarize, different studies already have proposed methods to reduce short, diurnal or seasonal solar power production variability.

Fewer studies have investigated in reduction of multiday solar power output variability from a meteorological standpoint. → expalain how? → 500hPa gph anomalies Cassou etc.

➔ Bloomfiled 2020 TCTs

➔ Thornton 2017

Grams *et al.* (2017) did but rejected the idea to further invest in it, based on their findings that it would need a tenfold increase of installed PV capacity in Europe to be comparable to the variability of wind power output. Therefore, they focused their study on wind and concluded, that spatial deployment of wind fleets based on information of different weather regimes can reduce the wind power output variability within Europe substantially. Nevertheless, they showed that connecting weather regime to PV power output variability is also possible. Even though the decision to focus on wind rather than solar power output variability is comprehendible, calculations of necessary future installed PV capacities gives reason to do the investigations anyway. Ram *et al.* (2017) estimated that the installed PV capacity for a 100% renewable scenario in Europe must rise to 1.94TW by 2050. The International Renewable Energy Agency (IRENA) estimated Europa's share a bit lower to 0.89TW. This is roughly a ten to twentyfold increase of installed PV capacity compared to the 87.19GW installed PV capacity used in Grams *et al.* (2017) study. Therefore, the impact of multiday PV power output variability caused by different weather regimes could also become substantial, which makes investigation of the optimal spatial deployment of future PV systems in Europe before further massive deployment of great interest. The results could support current planning activities and could help to reduce future grid balancing problems.

➔ Timescale discussion necessary?

- ➔ Stress events → example? Bloomfield 2018 2020 and der Wiel 2019
- ➔ Demand and production pattern → countries with highest demand and production
- ➔

IRENA 0.784TW EU and 0.107 rest of Europe

Short-term forecasting of solar power (PV) is much less developed as installed capacities are relatively small compared to installed wind power.

2. Data & Methods

Chapter 2 first describes the datasets which are the underlying sources of this study (section data). Afterwards it illustrates how the datasets are used to achieve the objective of reducing PV power output variability in Europe in the section method.

2.1 Data

2.1.1 ERA5

The reanalyse dataset, ERA5 (Hersbach et al., 2018), which is published by the European Centre for Medium-Range Weather Forecasts (ECMWF), is used as source for the weather regime definition. It provides atmospheric, land and oceanic variables from 1979 to present with a temporal resolution of an hour. The grid of ERA5 has a horizontal spatial resolution of 0.28 degrees (~31km) and 37 pressure levels in the vertical. A detailed documentation about ERA5 reanalyse dataset can be found on the ECMWF confluence web page (Hennermann & Yang, 2018).

We use the 500hPa geopotential height variable from ERA5 in the domain 80°W to 40°E, 30°N to 90°N. Geopotential height relates to low and high pressure systems (cyclones / anticyclones) and are commonly used for weather regime classification (Cassou, 2008; Grams et al., 2017; Michelangeli et al., 1995). The domain specification is reasonable for our meteorological field investigates since it captures the largescale circulation that affects Europe. The hourly dataset covers the time from 01.01.1979 until 31.05.2020, which yields in 363'048 datapoints. Additionally, the ERA5-Land (Muñoz Sabater, 2019) hourly data from 01.01.1981 until 31.05.2020 are used to get an overview of 2m temperature and surface solar radiation of the classified weather regimes. It is explicit designed for surface application and provides a more accurate dataset for this framework as ERA5. Especially over complex terrain (orography) the ERA5-Land adds value to the ERA5 surface field. Furthermore, ERA5-Land has a higher spatial resolution of 0.1 degrees (~9km) (Muñoz Sabater, 2019). We choose a slightly coarser resolution of 0.25 degrees, comparable to the 0.28 degrees of geopotential height.

2.1.2 Renewables.ninja and the Global Solar Energy Estimator (GSEE)

Renewables.ninja (www.renewables.ninja) is an interactive web platform that simulates hourly power output of wind and solar power plants all over the world. To calculate the PV power output, it uses the so-called Global Solar Energy Estimator (GSEE). The source code of the GSEE is freely available on GitHub and a detailed description of the GSEE can be found in Pfenninger and Staffell (2016). The theoretical background of the GSEE is based on Huld *et al.* (2010). The following variables are the key input parameter of this method to estimate the energy yield of PV modules:

1. Direct and diffuse irradiance at the PV panel
2. Panel temperature

Pfenninger and Staffell (2016) use three data sources to estimate these variables: The two reanalysis datasets of Modern-Era Retrospective analysis for Research and Applications (MERRA and MERRA-2) and the Surface Solar Radiation Data Set - Heliosat (SARAH). Figure 1 shows the general approach of GSEE.

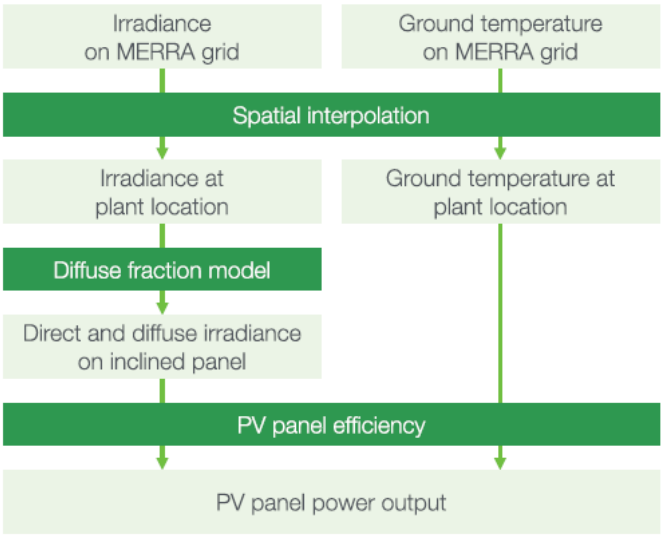

Figure 1: *Overview of the approach used to model PV power output* (Pfenninger & Staffell, 2016).

Since the estimates with MERRA are no longer provided by renewables.ninja we will hereafter only discuss the two datasets MERRA-2 and SARAH. Both are provided in hourly intervals from 1985-2016. SARAH is satellite-derived irradiance dataset with a high spatial resolution of 0.05° × 0.05° whereas MERRA-2 is a reanalysis dataset with a lower spatial resolution of 0.5° latitude and 0.625° longitude. MERRA only provides direct irradiance, but diffuse irradiance is needed as well. Therefore, they used the Boland-Ridley-Lauret model to estimate the diffuse irradiance (Ridley *et al.* 2010; Lauret *et al.* 2013). Since SARAH provides direct and global irradiance no further estimates were needed. Additionally, they use 2m temperature from MERRA-2 as estimates for the ambient temperature. To get the panel temperature they used the ambient temperature of MERRA-2 and additionally considered the effect of the irradiance on the panel temperature. This relation was estimated with site measurements of one of their sources (DTI see below). This dataset provides ambient and panel temperature for each site with which they derived an empirical relationship.

It is more common and easier to make comparison and analyses of PV power output with capacity factors rather than with absolute power output and we use this approach as well. The unit-less capacity factor CF is defined as:

$$CF = \frac{P}{IC} \qquad \text{Eq. 1}$$

where P is power output [W] and IC is the installed capacity [W].

MUSS MEHR KOMMEN

To evaluate the results obtained with the method described above, Pfenninger and Staffell (2016) compared it with capacity factors based on site measurements. To obtain the measured capacity factors they used three sources: DTI, PVLog.de and PVOutput.org. Over 1000 site data (measurements from PV systems) were collected from these three sources. Figure 2 shows a histogram of the difference between measured capacity factors and capacity factors simulated with the GSEE.

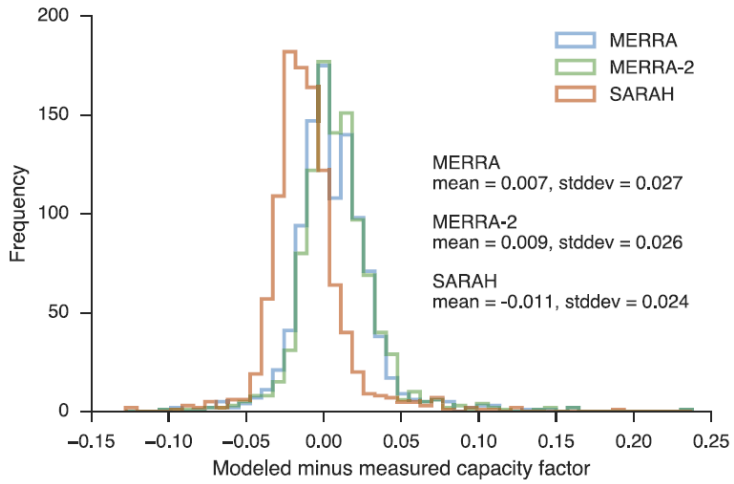

***Figure 2**: Histogram of the difference between the three modelled and measured capacity factors. Negative values infer underestimates of the capacity factor and positive values overestimates. The blue graph corresponds to modelled data with MERRA, the green graph to MERRA-2 and the red graph to SARAH. (Pfenninger and Staffell, 2016)*

The mean of this differences is taken by Pfenninger and Staffell (2016) as basis for a bias correction. They used it to calculate one correction factor for each simulation (MERRA, MERRA-2 and SARAH).

Additionally to the power output simulation of a wind or solar plant at a specific location, renewables.ninja also provides capacity factors per country. Pfenninger and Staffell (2016) have performed randomized (tilt and azimuth angel) national-scale simulations with MERRA-2 and SARAH data to estimate averaged capacity factors per country. Also, these data were analysed against the measured site data. The measured capacity factor per country was then calculated as the mean of all capacity factors per site in one country.

This capacity factor per country suits perfect for our need of analyizng PV power output variability and its reduction potential.

But one must consider that this is strongly depended on the amount and position of measurement sites in a country. For example, for Spain they only have 14 available measurement sites that are mostly located at the northern coast. This leads to a statistically unrepresentative sample (Pfenninger & Staffell, 2016).

Nevertheless, a further advantage of this approach is to be in line with the study of Grams *et al.* (2017) which makes further comparison or combination analyses of wind and solar power output variability easier.

We use the capacity factor per country within our thesis to achiev the goal of reduction of PV power output variability within Europe.

Since our study focusses on the reduction of PV power output variability within Europe, we operate with rather large-scale and long-term quantities. Therefore we make use of the capacity factors per country by Pfenninger and Staffell (2016)

We use this capacity factor per country to achieve the goal of reducing the PV power output variability. The benefits from SARAH are the higher spatial resolution and it is more precise in estimating the energy yield of PV panels on hourly to daily time scales than MERRA-2 (PFENNINGER). But it suffers from a significant amount of missing data. Especially prior to 1995 the lack of data prevents long-term consistency.

2.1.3 Installed PV capacities

Data from the International Renewable Energy Agency (IRENA) are used to gather the current installed PV capacities (2019) for each country in Europe. *"IRENA is an intergovernmental organisation that supports countries in their transition to a sustainable energy future, and serves as the principal platform for international co-operation, a centre of excellence, and a repository of policy, technology, resource and financial knowledge on renewable energy"* (IRENA, 2020b). The used data can be found in the "Renewable Capacity Statistics 2020" report by IRENA. Together with the capacity factors by renewables.ninja (section 2.1.2) the PV power output for each country are calculated (Eq. 1). Furthermore, the estimates "where we need to be" in 2050 presented in the "Energy Transformation Roadmap to 2050" by IRENA are used as one source for the PV installed capacity in Europe 2050 (IRENA, 2020a). The other sources to estimate the needed PV IC in 2050 are the Energy Watch Group (Ram et al., 2017) and SolarPower Europe (SolarPower Europe and LUT University, 2020).

To further analyse where the PV power output variability is heading to, the National Energy and Climate Plans (NECPs) of each country in the EU are used. Within the NECPs each country defines the amount of PV systems they plan to install until the year 2030. For the rest of Europe individual national plans are considered or if not found the average PV installed capacity growth rate until the year 2030 from all EU countries is multiply with the current PV installed capacity to get an estimate.

2.1.4 Electricity consumption data

Electricity consumption data are taken from the open-power-system-data (opsd). For countries which are missing in the opsd dataset, the statistical office of the European Union (Eurostat) is used as source. Since the availability of the data per year differs per country, we take the latest fully reported year for each country as current total electricity consumption (range between 2016 and 2019).

➔ Table with all IC per country? Consumption? Only countries?

2.2 Method

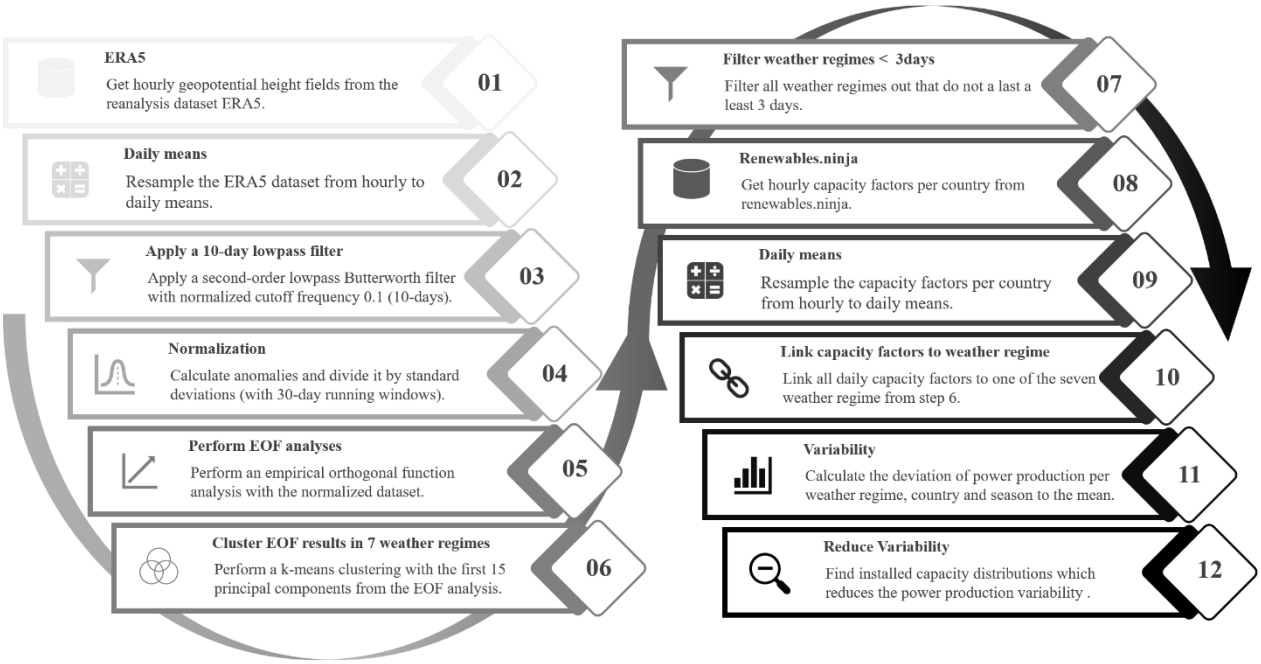
ERA5
Get hourly geopotential height fields from the reanalysis dataset ERA5.
01
Daily means
Resample the ERA5 dataset from hourly to daily means.
02
Apply a 10-day lowpass filter
Apply a second-order lowpass Butterworth filter with normalized cutoff frequency 0.1 (10-days).
03
Normalization
Calculate anomalies and divide it by standard deviations (with 30-day running windows).
04
Perform EOF analyses
Perform an empirical orthogonal function analysis with the normalized dataset.
05
Cluster EOF results in 7 weather regimes
Perform a k-means clustering with the first 15 principal components from the EOF analysis.
06
Filter weather regimes < 3days
Filter all weather regimes out that do not a last a least 3 days.
07
Renewables.ninja
Get hourly capacity factors per country from renewables.ninja.
08
Daily means
Resample the capacity factors per country from hourly to daily means.
09
Link capacity factors to weather regime
Link all daily capacity factors to one of the seven weather regime from step 6.
10
Variability
Calculate the deviation of power production per weather regime, country and season to the mean.
11
Reduce Variability
Find installed capacity distributions which reduces the power production variability .
12

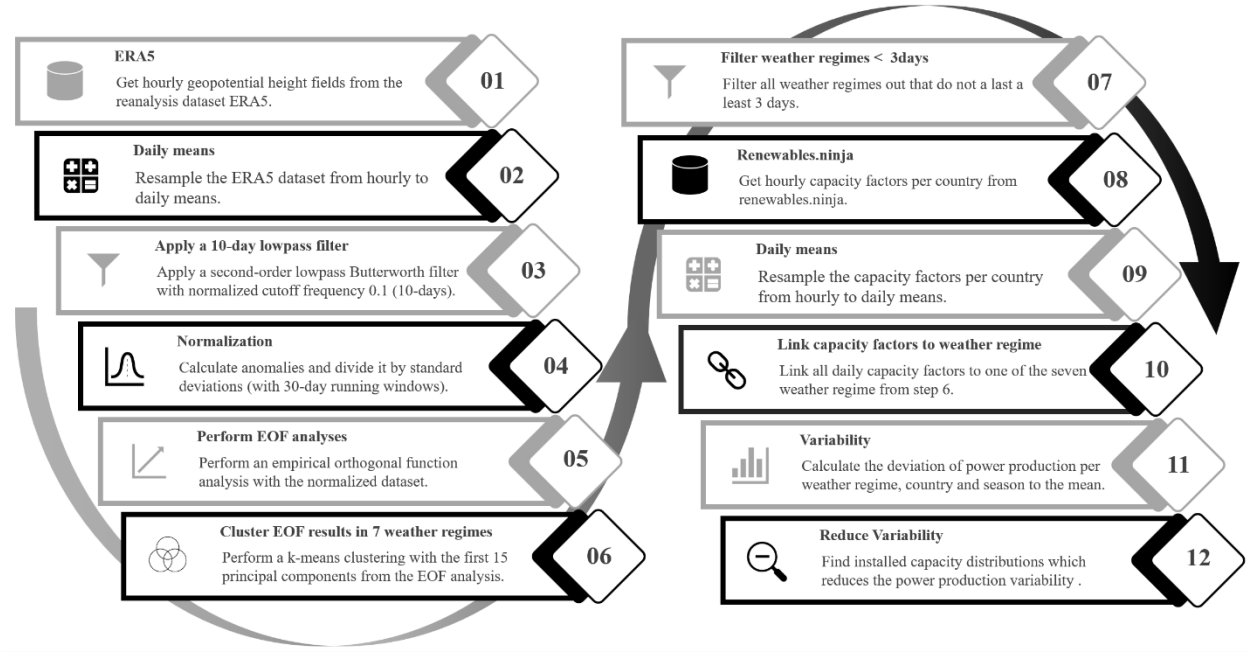
ERA5
Get hourly geopotential height fields from the reanalysis dataset ERA5.
01
Daily means
Resample the ERA5 dataset from hourly to daily means.
02
Apply a 10-day lowpass filter
Apply a second-order lowpass Butterworth filter with normalized cutoff frequency 0.1 (10-days).
03
Normalization
Calculate anomalies and divide it by standard deviations (with 30-day running windows).
04
Perform EOF analyses
Perform an empirical orthogonal function analysis with the normalized dataset.
05
Cluster EOF results in 7 weather regimes
Perform a k-means clustering with the first 15 principal components from the EOF analysis.
06
Filter weather regimes < 3days
Filter all weather regimes out that do not a last a least 3 days.
07
Renewables.ninja
Get hourly capacity factors per country from renewables.ninja.
08
Daily means
Resample the capacity factors per country from hourly to daily means.
09
Link capacity factors to weather regime
Link all daily capacity factors to one of the seven weather regime from step 6.
10
Variability
Calculate the deviation of power production per weather regime, country and season to the mean.
11
Reduce Variability
Find installed capacity distributions which reduces the power production variability .
12

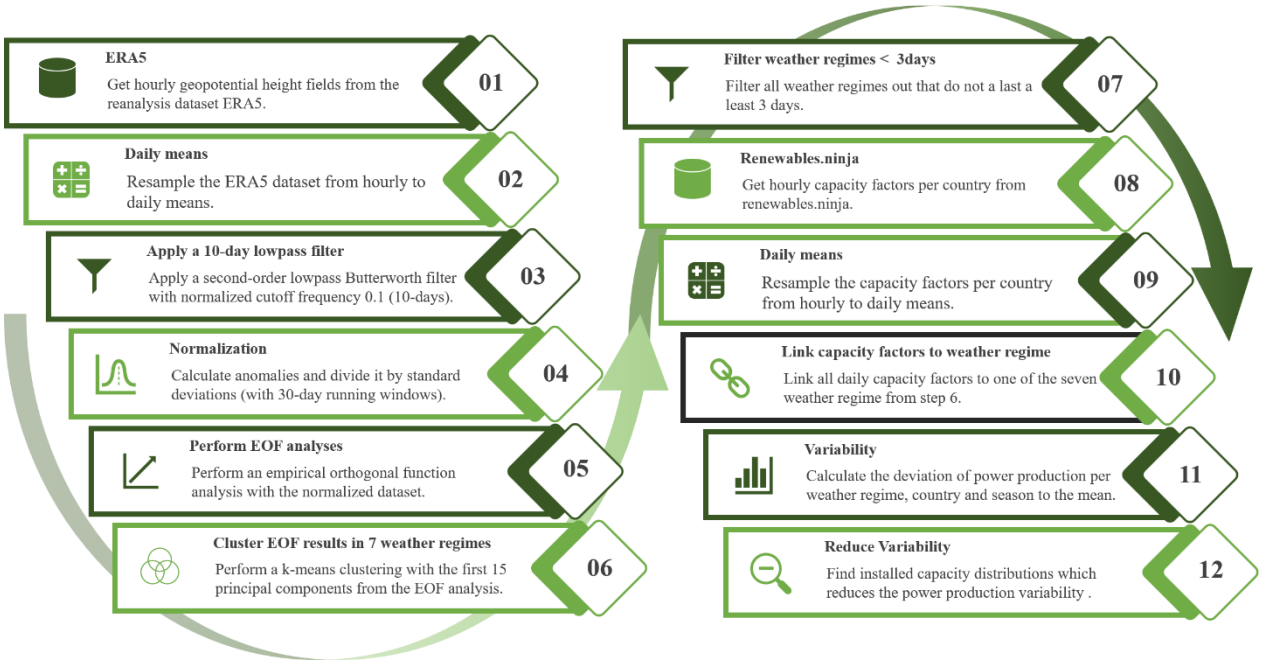

2.2.1 ERA5 data pre-processing

As first step the hourly geopotential height fields from ERA5 are resampled by calculating daily means because weather regimes typically last several days, and an hourly temporal resolution is not necessary. Furthermore, a 10-day lowpass filter is applied to smooth the data. The input data for the EOF analysis (see section 2.2.2) are standardized anomalies which are calculate with the lowpass filtered daily means:

$$std\_ano_d = \frac{z_d - z_{d,mean}}{z_{d,std}} \qquad \text{Eq. 2}$$

where z_d are the lowpass filtered daily means of the geopotential height, $z_{d,mean}$ is the climatological mean with a running window of 30 days, and $z_{d,std}$ is the standard deviation of the geopotential height with a running window of 30 days. The running window is defined such as the respective day acts as centre of the window. For instance, to derive the reference climatology for the 15th of January the mean of the first to the 30th January is calculated for every year and grid point. This results in 41 means per grid point since our dataset covers 41 years. These 41 means per grid point are taken again to calculate a mean, so that we finally have one reference climatology for the 15th of January for every grid point. This is done analogous for every day of the year, which yields in 366 sperate reference climatology and standard deviations.

Standardized anomalies are used because of the weather regimes definition year around. Since it includes normalizing with the standard deviation, the amplitude in the anomaly caused by the seasonal cycle is removed prior to the weather regime classification. The used 30-day running window for the reference climatology and standard deviation calculations differs to other studies. Often, investigations are only made

for weather regime in winter where a correction for the seasonality is not needed (REF). Others (GRAMS) are using 90-day but since our interest focus on multiday timescale this is rather long and increases the probability that the impact of the signal of the seasonal cycle is rather high.

EVTL PICTURES WITH COMPARISON

2.2.2 Weather regime classification

For the weather regime classification, the well-known method of empirical orthogonal function analysis and k-means clustering is used (Cassou, 2008; Michelangeli et al., 1995). An EOF analyses decomposes a dataset into statistically orthogonal modes that describe the variability of the data. For metrological datasets, a few modes are often sufficient to explain a large fraction of the total variability in the data, which is helpful to assess the key patterns of the variability and to further analyse them. We perform the EOF analysis on our pre-processed data with the eofs python package by Dawson (2016).

The resulting first 16 principal components of our EOF analyses, which explained ~90% of the variance, are used to cluster the data into weather regimes. We use the clustering method k-means which is implemented in the python package sklearn.cluster by Pedregosa *et al.* (2011). Generally, clustering techniques are used to group data with similar characteristics by minimizing the variance within the clusters. The difficulty lies in the definition of the number of clusters. For the Euro-Atlantic region often four clusters are used to define the weather regimes (Cassou, 2008; Michelangeli et al., 1995; van der Wiel et al., 2019). The well-studied four weather regimes which are received with this approach are the negative and positive phase of the North Atlantic Oscillation, the Scandinavia high and the Atlantic ridge (EVTL FIG). But most of these studies focus only on wintertime weather regime classification. According to Grams *et al.* (2017) the optimal number of clusters to define weather regime year around is seven which seems to be plausible by a simple check with the elbow and silhouette method (EVTL FIG). Therefore, we use 7 clusters as well which additionally make a comparison/combination with the study by Grams *et al.* (2017) easier. Furthermore, we sort all days out where the weather regime does not last at least 3 days and assign these days to a separate weather regime hereafter called “no-regime”.

To summaries, we use EOF analyses and k mean clustering to derive an assignment for each day of the ERA5 dataset to one of 7 weather regime or to no-regime.

2.2.3 Capacity factors

The national aggregated CF by renewable.ninja are used, which are provided in hourly intervals. The advantage of this dataset is the included bias correction described in section 2.1.2.

The CF dataset is resampled analogously to the ERA5 dataset to get daily means. Since the CF are highly influenced by the seasonal cycle, they are analysed separately for each season (winter, spring, summer, autumn) (EVTL FIG OF HISTOGRAMM). Together with the weather regime classification, the capacity factor can now be attributed to different weather regimes. The attributed capacity factors are used

to calculate a mean capacity factor per weather regime, season, and country. The difference between this mean capacity factors and the mean capacity factors for the whole season of a country determines whether the impact of the weather regime exhibits over- or underproduction (Eq. 3).

$$\Delta CF_{wr,country,season} = CF_{wr,country,season} - CF_{country,season} \quad \text{Eq. 3}$$

where $CF_{wr,country,season}$ is the mean capacity factor of a specific weather regime, country and season [unitless] and $CF_{country,season}$ is the mean capacity factor of a country for the whole season [unitless].

Multiplication of capacity factors with installed capacities yields power output (Eq. 1). This can be used to expand Eq. 3 which gives the total deviation of solar power output of Europe per weather regime and season.

$$\Delta P_{wr,Europe,season} = \sum_{country} \left(\Delta CF_{wr,country,season} * IC_{country}\right) \quad \text{Eq. 4}$$

where $IC_{country}$ is the installed capacity per country [W] and $\Delta CF_{wr,country,season}$ is the deviation of CF per weather regime, country and season to the seasonal mean [unitless].

Eq. 4 is used as an expression for the variability. If the result of this equations is zero, the PV power production of the respective weather regime and season is equal to the mean PV power production of the respective season and therefore the variability is maximally reduced.

→Explain plot for total variability.

2.2.4 Variability reduction with optimal IC distribution

To determine an IC distribution which distinctive reduces the PV power generation variability, Eq. 4 for every country, season and weather regime is used in a linear least-square problem with an upper and lower bound on the variables. This is done with the scipy.optimize.lsq_linear python package which solves the following optimization problem:

$$\begin{aligned} &\text{minimize } 0.5 \times ||\mathrm{A}\vec{\mathrm{x}} - \vec{\mathrm{b}}||^2 \\ &subject\ to\ lb \leq x \leq ub \end{aligned} \quad \text{Eq. 5}$$

where A is the coefficient matrix, x is the solution found, b is the target vector, lb is the lower bound of the solution x and ub is the upper bound of the solution x.

The coefficient matrix A is defined with $\Delta CF_{wr,country,season}$ from Eq. 3 the following:

$$A = \begin{pmatrix} \Delta CF_{WR0,AL,winter} & \cdots & \Delta CF_{WR0,SK,winter} \\ \vdots & \ddots & \vdots \\ \Delta CF_{WRX,AL,autumn} & \cdots & \Delta CF_{WRX,SK,autumn} \end{pmatrix} \quad \text{Eq. 6}$$

where the first element of the matrix $\Delta CF_{WR0,AL,winter}$ is the capacity factor anomaly of weather regime 0, in the Albanian winter. The country persists per column, but it goes through all weather regimes (0-7) and seasons, which gives a total of 32 rows. Per row the matrix goes through all countries, from Albania to Slovakia, which results in 36 columns for the considered countries defined above (→ define somewhere above → table with current IC per country!?).

The target vector $\vec{b}$ is set to zero to reduce the variability within one weather regime and season as much as possible and therefore also reduces the variability from one weather regime to other:

$$\vec{b} = \begin{matrix} 0 \\ \dots \\ 0 \end{matrix} \quad \text{Eq. 7}$$

where $\vec{b}$ has the same length as the number of rows of matrix A.

The result of this method is the vector $\vec{x}$ which contains then the IC for each country:

$$\vec{x} = \begin{matrix} IC_{AL} \\ \dots \\ IC_{SK} \end{matrix} \quad \text{Eq. 8}$$

The method to perform the minimization is the Trust Region Reflective (TRF) algorithm (Branch et al., 1999).

The lower bound is always set to the current (2019) PV IC per country (unless something else is mentioned in the scenarios below). The upper bound is always set to the potential PV IC which is taken from the study by → JAN FRAGEN/NACHSHAUEN PAPER

2.2.5 Scenarios

This section describes the expansion of the method in section 2.2.4 to depict different scenarios for future PV IC distributions. The underlying goal of all scenarios is to reduce the PV power generation variability but with different constraints. The different constraints are added row/element wise to the coefficient matrix A (Eq. 6) and the target vector $\vec{b}$ (Eq. 7). The newly added rows and elements act as additional equations within our linear least-square problem and their residuals are consequently also minimized.

To meet the requirements of the different scenarios described below and get a better control over our linear least-square problem, we introduce a weighting vector $\vec{w}$:

$$\vec{w} = \begin{matrix} w_0 \\ \cdots \\ w_x \end{matrix} \qquad \text{Eq. 9}$$

where the elements of the vector $\vec{w}$ are the weightings for each of our equations defined with the coefficient matrix A and the target vector $\vec{b}$. The weighting vector is also useful to consider the various orders of magnitudes of our equations. I.e., the first 28 rows are of the same order of magnitude because they all describe the PV power output variability. But this is not the case if we introduce an equation/row which constrains our system to a minimum total European PV power production. Additionally, it must be considered that the method used to solve the linear least-square problem, minimizes the sum of the residuals of the equations. Since our first 32 equations are all about the variability they are already relatively highly weighted compared to one equation we add. With the introduced weighting vector, it is possible to counteract and give more weight to the one added equation if necessary.

To apply the weighting vector to the linear least square problem the square root of its elements is taken as elements of a diagonal matrix and multiplied with the coefficient matrix A and the target vector $\vec{b}$ before the optimization problem is solved. → EQ AUFSCHREIBEN!?

2.2.5.1 Scenario 1 (S1) – PV power production and installed capacities from NECPs 2030

The objective of S1 is to minimize the PV power production variability but the total installed capacities and power production with PV systems in Europe must equal (+/- 1GW) to the ones we estimate if the NECPs for 2030 are fulfilled. This gives a direct comparison of the variability estimated with the plans of the countries in Europe for 2030 to the variability reduction potential we have if distribute the same additional amount optimally to reduce the variability.

To realize S1 two rows and elements are added to the coefficient matrix A and the target vector $\vec{b}$, respectively. The first row adds the constraint that the total IC must be equal to the total IC planned for 2030. This is achieved by adding a row with ones to the coefficient matrix A and the total IC planned for 2030 as element to the target vector $\vec{b}$. The second row considers for the total PV power production. PV power production is calculated by multiplying IC with the CF (Eq. 1). Therefore, we add all the mean CF per country as row to the coefficient matrix A. The total PV power production is added to the target $\vec{b}$. It is calculated as sum of the CF per country multiplied by the planned IC per country for 2030.

$$A_{S1} = \begin{pmatrix} \cdots & \cdots & \cdots \\ 1 & \ddots & 1 \\ CF_{AL} & \ddots & CF_{SK} \end{pmatrix} \qquad \text{Eq. 10}$$

where A_{S1} is the coefficient matrix for S1 (expansion of Eq. 6) and CF_{AL} and CF_{SK} are the mean capacity factors for Albania and Slovakia which represents the mean CF for all countries.

$$\overrightarrow{b\_S1} = \begin{matrix} \dots \\ tot_{IC\_2030} \\ tot_{production\_2030} \end{matrix} \quad \text{Eq. 11}$$

where b_S1 is the target vector for S1 (expansion of Eq. 7), tot_{IC_2030} is the total installed capacity planned for 2030 and $tot_{production\_2030}$ is the total PV power production estimated with the planned IC 2030. The weighting vector for S1 is chosen such that all the equations which consider for the variability are set to one. The weighting of the equation which considers for the total IC are set to XY and the equation which considers for the total PV production is set to XY.

2.2.5.2 Scenario 2 (S2) – PV IC in 2050

In S2 estimates of PV IC for the year 2050 are taken and used as additional equation in our linear least-square problem. Similar as in S1 it is achieved by adding a row with ones to the coefficient matrix A and the total PV IC estimates for 2050 as element to the target vector $\vec{b}$. The following table shows estimates by three different sources for the needed PV IC in the year 2050:

Table 1 Estimates of needed installed PV capacities for the year 2050.

Source	PV IC 2050 estimate [TW]	Comment / Scenario
SolarPower Europe	4.7 – 8.8	4.7 TW in the Laggard scenario, 7.7 TW in the Moderate scenario and 8.8 TW in the Leadership scenario
IRENA	0.891	REmap Case
Energy Watch Group	1.94	100% RES scenario of the Energy

S2 is calculated twice, first with lowest values from Table 1 estimated by IRENA with 0.891 TW and second with the highest values estimated by SolarPower Europe in their Leadership scenario with 8.8 TW. The weighting vector for S1 is chosen such that all the equations which consider the variability are set to one and the equation for the total PV IC is set to XY.

To set the results into context the variability is also calculated with the same amount of PV IC but percentual equally distributed to the countries as it was in the year 2019 (or better the ones which are planned for 2030?).

2.2.5.3 Scenario 3 (S3) – Cost minimization

Additionally to the PV power output variability reduction, S3 focuses on minimizing the costs. This is done by minimizing the amount of PV IC with the constraint that they must produce the same amount of electricity as estimated with the PV IC planed in the NECPs for 2030. This leads to the to same expansion of our method as described in S1 but instead of adding the total IC planned for 2030 as element to the target vector $\vec{b}$ it is now set to 0.

The weighting vector for S3 is chosen such that all the equations which consider the variability are set to one. The weighting of the equation which considers for the total IC are set to XY and the equation which considers for the total PV production is set to XY.

2.2.5.4 Scenario 4 (S4) – Cover XY% of country specific consumption with PV systems

The objective of S4 is to minimize the PV power production variability but each country must generate XY% of its electricity consumption with PV systems. The latest (between 2016 and 2019) available yearly electricity consumption data (section 2.1.4) is taken as source for this purpose. Projections of electricity consumption to for the year 2030 are neglected. S4 is constructed like S1 but instead of the current PV IC for each country as lower bound, S4 uses XY% of the yearly consumption per country divided by the CF per country as lower bound.

$$lb_{country} = 25\% \times \frac{load_{country}}{CF_{country} * 365d * 24\frac{h}{d}} \quad \text{Eq. 12}$$

where $lb_{country}$ is the lower bound for PV IC per country [W], $load_{country}$ is the yearly electricity consumption per country [Wh] and $CF_{country}$ is the capacity factor per country [unitless].

3. Results

Chapter 3 gives an overview of the obtained results. First, it describes the derived weather regimes and the linked capacity factors anomalies per country and season. Second, the results of the scenarios and their installed PV capacity distributions and variability are presented.

3.1 Weather regimes and their linked capacity factor anomalies

Figure 3 gives an overview of the derived weather regimes and their relation to the two most important input variables for the GSEE. Namely the surface solar radiation and the 2m temperature. In Figure 3a) the weather regimes are presented as standardized geopotential height anomalies and their frequency of occurrence. A more detailed overview of their frequency can be found in Figure 5. Surface solar radiation and 2m temperature are also presented as standardized anomalies in Figure 3b) an Figure 3c) respectively. The relation between the weather regime number and the ordinary names, which are often used in literature, can be found in Table 2.

The link between the weather regimes and the derived capacity factor anomalies are shown in Figure 4. The first row of Figure 4 shows again the seven weather regimes plus no regimes. Beneath the weather regimes, in the same column, the corresponding country specific capacity factor anomalies can be found. The different seasons are shown separately from winter (December, January, February → DJF), to spring (March, April, May → MAM), to summer (June, July, August → JJA), to autumn (September, October, November → SON). The capacity factor anomalies are calculated as difference to the corresponding seasonal mean.

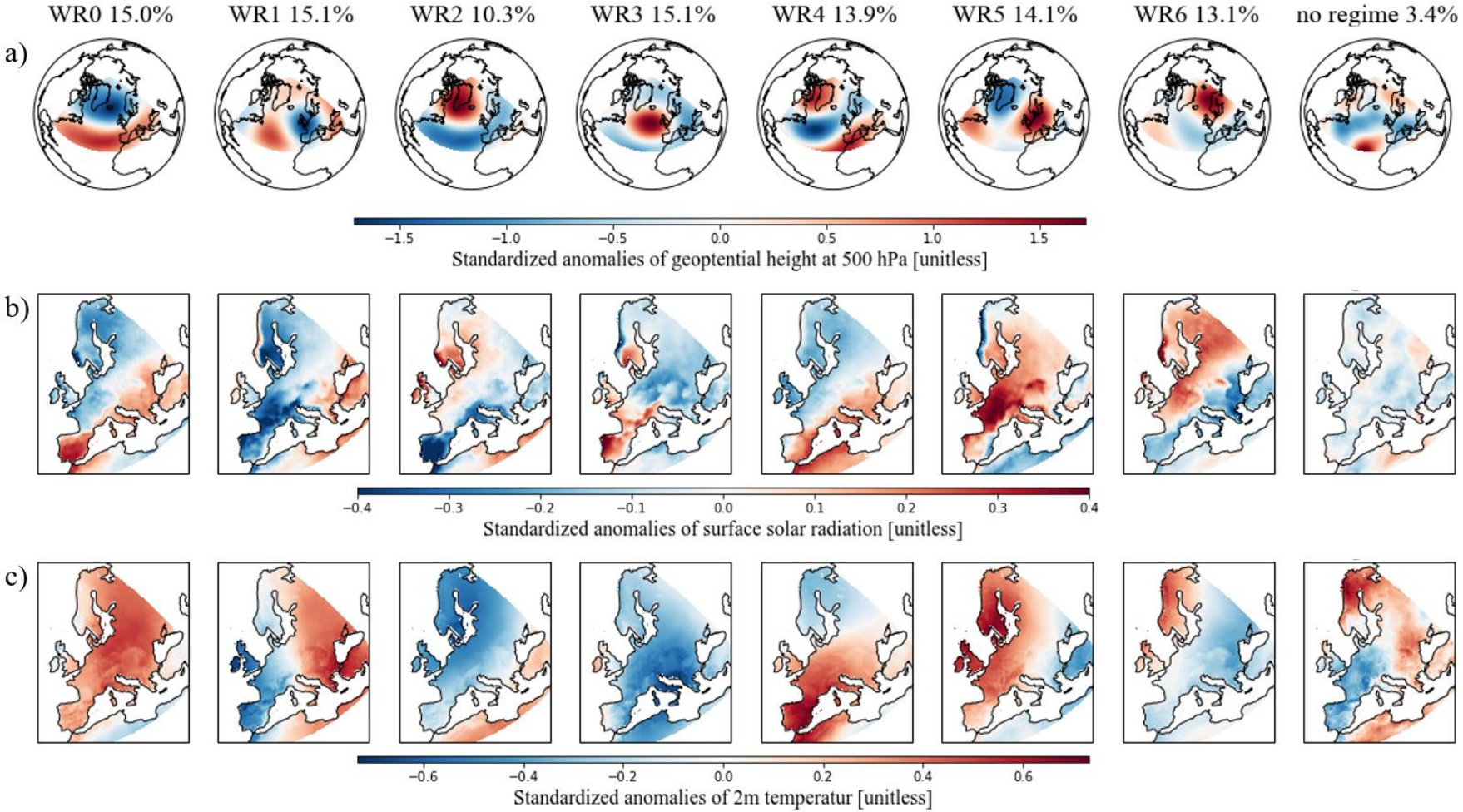

Figure 3: Different variables of the derived seven weather regimes and no regime plus their frequency of occurrence. a) Standardized anomaly fields of geopotential height at 500 hPa. b) Standardized anomaly fields of surface solar radiation. c) Standardized anomaly fields of 2m temperature.

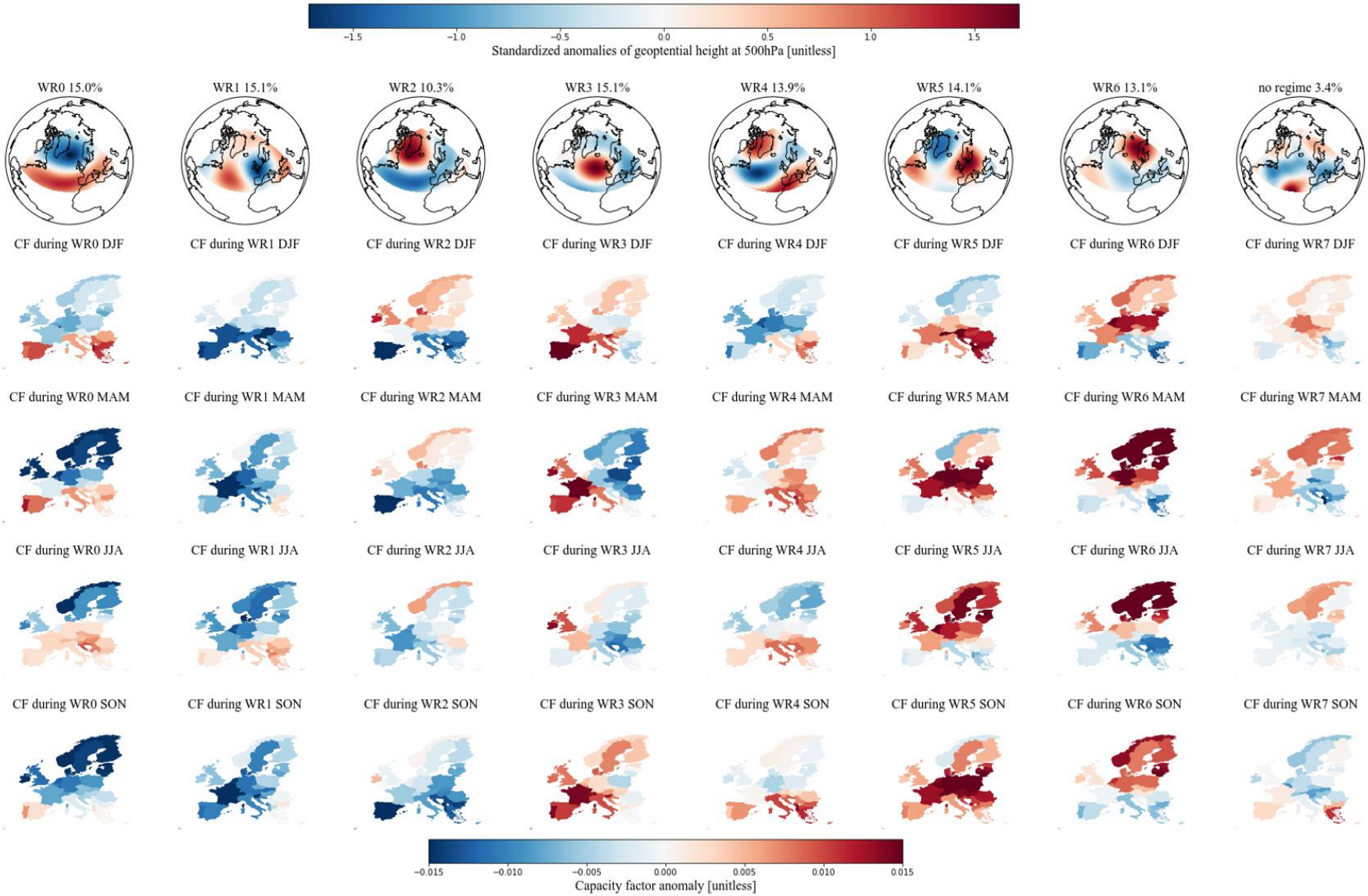

Figure 4: Link between the derived seven weather regimes (WR) and the capacity factor (CF) anomalies per country and season. The first row shows standardized anomaly fields of geopotential height at 500 hPa for each weather regime. The linked capacity factor anomalies per country are shown separately for each season and are calculated as difference to the corresponding seasonal mean: Winter (DJF), spring (MAM), summer (JJA) and autumn (SON).

Table 2: Relation between weather regime numbers and ordinary weather regime names.

WR0	Positive phase of the North Atlantic Oscillation (NOA+)
WR1	European trough
WR2	Negative phase of the North Atlantic Oscillation (NOA-)
WR3	Atlantic ridge
WR4	Atlantic trough
WR5	European blocking
WR6	Scandinavian blocking

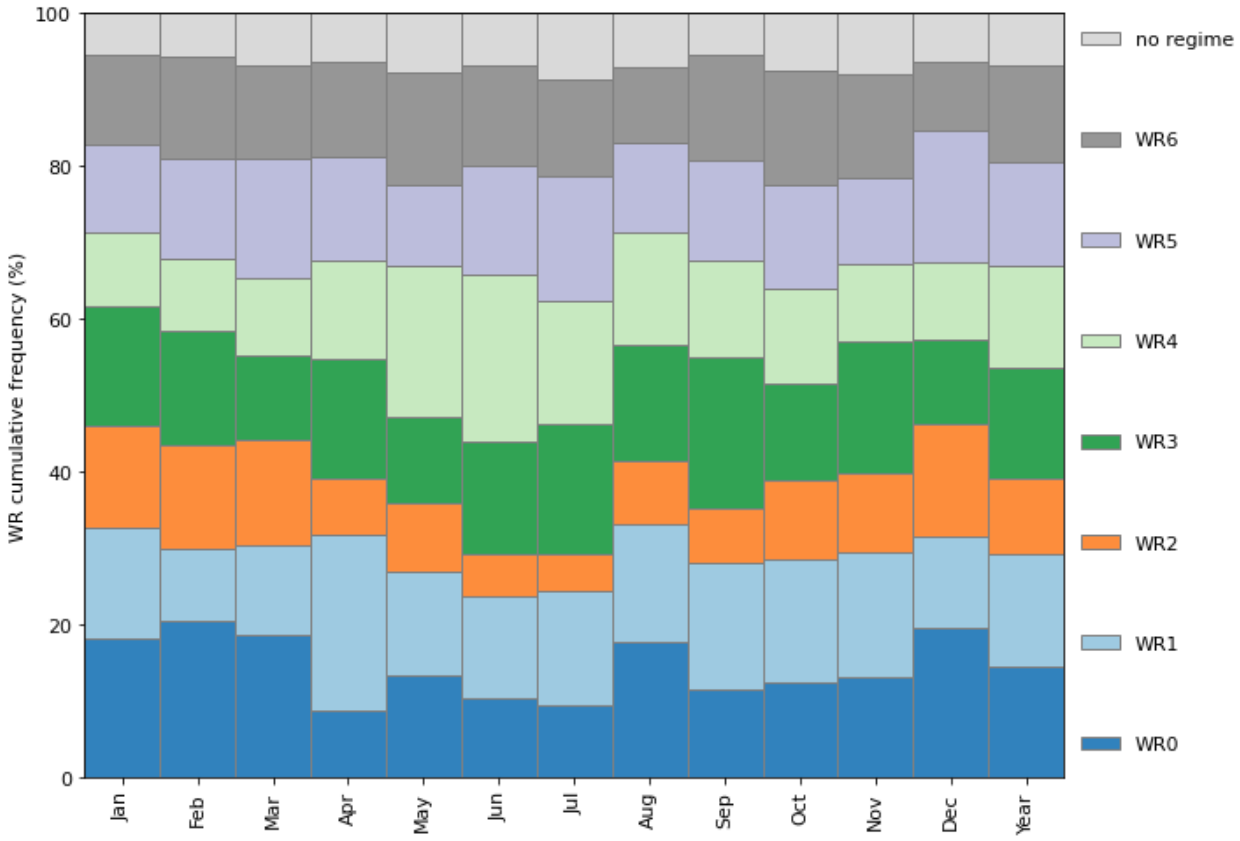

Figure 5: Cumulative frequency of the seven weather regimes (WR) and no regime.

3.1.1 Weather regime 0 / NOA+

WR0, the positive phase of the NOA, shows a negative geopotential height anomaly (cyclone) over the Northern part of the Atlantic and a positive geopotential height anomaly (anticyclone) over the Atlantic/Mediterranean sector. During this conditions, the Atlantic storm tracks are displaced North-eastward, and the zonal flow is enhanced. This increases the strength of the westerlies and brings maritime air (warm and moist) to Central and Northern Europe (Hurrell et al., 2003; Rogers, 1997; Wallace & Hobbs, 2006). Consequently, the storm track activity over Northern Europe is enhanced, which implies a larger cloud clover fraction and therefore less available surface solar radiation. Studies by Pozo-Vázquez *et al.* (2004; 2011) indeed have shown that that the NOA index is negatively correlated with the surface solar radiation in Northern Europe and positively correlated with surface solar radiation in southern Europe. Our results agree with these studies with negative surface solar radiation anomalies in Northern Europe, positive surface solar radiation in Southern Europe and positive temperature anomalies almost all over Europe (Figure 3b) and c), first column).

The CF anomalies during the positive phase of the NOA also exhibit a clear North to South discrepancy. Northern Europe shows negative CF anomalies whereas Southern Europe is dominated by positive CF anomalies. This is in line with the surface solar radiation described above but its limpidity changes throughout the season. I.e., in spring (MAM) the results show a strong and clear difference between Southern and Northern Europe. But in autumn (SON) only the Iberian Peninsula and a few Countries in South-eastern Europe exhibit positive CF anomalies. WR0 is more frequent during winter times which may explain the change of the limpidity in the discrepancy (Figure 5).

3.1.2 Weather regime 1 - European trough

WR1, the European through, is characterized by a meridional dipole of a positive and negative geopotential height anomaly in the Atlantic and Western Europe, respectively. The cyclone located over Western Europe brings relatively warm air from the South to South-eastern Europe and higher temperature than normal can be observed (Figure 3c), WR1). Surface solar radiation anomalies are also enhanced in South-eastern Europe but are not as pronounced. Western Europe, where the cyclone is located at, shows negative temperature and surface solar radiation anomalies expect the Northern part of the British Isles and the Western coast of Norway, which is already on the northern edge of the cyclone.

The CF anomalies during the European trough are mostly negative. Especially in winter (DJF) where Southern and South-eastern Europe exhibit an even larger negative impact than Northern Europe. Interestingly, this weakens in spring even turns to positive CF anomalies in summer which is more in line with our surface solar radiation anomalies presented year around. This may be caused because WR1 is less frequent in winter than summer and spring (Figure 5).

3.1.3 Weather regime 2 – NOA-

WR2, the negative phase of the NOA, exhibits contrary geopotential height anomaly fields than the positive phase of the NOA. It is characterized by a negative geopotential height anomaly over the Atlantic/Mediterranean sector and positive geopotential height anomaly over Greenland. This also yields in reversed surface weather variables than the positive phase of the NOA. More available surface solar radiation than the climatological average in Northern Europe and lower surface solar radiation in Southern Europe. The temperature anomalies are negative all over Europe.

The contrary pattern to the positive NOA is also reflected in the CF anomalies with positive values in Northern Europe and negative values in the South. But we can see here as well that this discrepancy between North and South is clear in winter and spring but weakens in summer and autumn where more negative CF anomalies are present in Northern regions. Again, the cause my lie in the more frequency occurrence of WR2 during winter times (Figure 5).

3.1.4 Weather regime 3 - Atlantic ridge

WR3, the Atlantic ridge, exhibits a strong positive geopotential height anomaly (anticyclone) over the Atlantic. Enhanced surface solar radiation anomalies can be seen in Western Europe, mainly over the Iberian Peninsula and over Southern Scandinavia. These regions are located at the western edge of the anticyclone. This could explain the enhanced surface solar radiation because of the relation between anticyclones and descending air and therefore clear sky conditions. Eastern Europe, which is already outside the region of the anticyclone, shows negative surface solar radiation. The anticyclone brings relatively cold air from the North to Europe and therefore one can observe negative temperature anomalies all over Europe expect the Western coast of Iberian Peninsula and the British Isles.

The East-West gradient is also visible in the CF anomalies. With positive anomalies in the West and negative anomalies in the East. But the seasonal differences are substantial. In spring (MAM) one can observe a strong East-West gradient. In winter (DJF) and autumn (SON) one can still see a discrepancy between East and West but the anomalies are less enhanced and generally more often positive. The opposite is the case for summer where one can see more often but less enhanced negative anomalies but still with an East-West gradient.

3.1.5 Weather regime 4 - Atlantic trough

WR4, the Atlantic, trough, shows a meridional dipole pattern of the geopotential height anomaly reversed to WR1. But the cyclone and anticyclone are more elongated in meridional direction. The negative anomaly is located over the Atlantic and Northern Europe and the positive anomaly is located over the Mediterranean sector. It can be best compared with the Atlantic trough weather regime (i.e. GRAMS) but the positive geopotential height anomaly over South-eastern Europe does not fit well to this association. WR4 exhibits enhanced temperature anomalies over Southern and Central Europe in the region of the

positive geopotential height anomaly and slightly negative temperature anomalies over Scandinavia. The surface solar radiation anomalies show a clear gradient from South-Eastern to North-Western Europe. Positive values are located over the Mediterranean region and negative values anomalies over Scandinavia and British Isles.

The CF anomalies of the countries in the Mediterranean region are like to the surface solar radiation anomalies and show mostly slightly positive values. In Northern Europe, the difference between the season is more pronounced. In winter and summer, they are negative but in autumn and especially in spring more Northern countries exhibits positive CF anomalies.

3.1.6 Weather regime 5 - European blocking

WR5, the European blocking, shows a positive geopotential height anomaly (anticyclone) over Central Europe. This is associated with descending air which brings clear skies over central Europe and therefore enhanced surface solar radiation anomalies can be observed in Figure 3b, WR5. Only in the Scandinavian region and in Eastern Spain it is less pronounce or even negative because these regions are already on the edge of anticyclone. The temperature is also enhanced especially in North-Western Europe which is the region where the anticyclone brings warm air from the South northwards.

With the clear sky and warm temperature, the CF are also higher than normal. Greatly increased CF anomalies can be observed especially in central Europe. In winter, the CF anomalies are only negative for Scandinavia and the British Isles. Towards summer these changes to positive CF anomalies whereas it changes for Southern countries to negative CF anomalies.

3.1.7 Weather regime 6 - Scandinavian blocking

Like the European blocking the positive geopotential height anomaly (anticyclone) over Scandinavia relates to descending air, which results in clear sky condition and therefore enhanced surface solar radiation (Figure 3b, WR6). Since the anticyclone is now located more to the North, Southern countries exhibit less surface solar radiation than normal. The positive temperature anomalies have now also shifted Northwards to the Scandinavian region. The anticyclone brings relatively cold air from the North to South-eastern Europe where a negative temperature anomaly can be observed (Figure 3c), WR6).

The CF anomalies show greatly increased values over Northern Europe throughout the whole year whereas the CF anomalies in Southern Europe are lower than normal.

3.1.8 No regime

No regime (weather regimes that no not last at least 3 days) does not show a clear structure (cyclone and/or anticyclone) as WR0 to WR6 expect half of an anticyclone (due to the domain definition) in the Atlantic. Other than this anticyclone, slightly negative geopotential height anomalies dominate over the Atlantic and Southern and Central Europe. Slightly positive geopotential height anomalies can be observed

in Northern Scandinavia. The anomalies are not very pronounced, which we could expect because it is the average of different weather regimes. Also, the surface solar radiation is not very pronounced but slightly negative. The 2-m temperature shows similar distribution as the geopotential height anomaly with positive values and Northern-eastern Europe and negative values in South-western Europe.

Also, the CF anomalies are not very pronounced but with slightly positive values in Northern Europe and slightly negative values in Southern Europe in winter, spring and summer. In autumn it changes, and Northern Europe has mostly slightly negative CF anomalies where Southern Europe shows more positive values.

The frequency of no regime amounts to 3.4% which indicates that only 3.4% of all analysed days are not linked to a weather regime.

3.2 Installed capacity distributions and their variability

We hereafter present the results of the various scenarios with their IC distributions and PV power output variability. To put the results in context, they are always shown together with the IC distributions and variability of the year 2019 (Figure 6, first plot) and/or the IC distribution and variability which we estimate for the year 2030 if the plans from NECPs are fulfilled (Figure 6, second plot).

The total IC in Europe in the year 2019 was 131.2 GW (IRENA, 2020b). Its distribution is presented in the first plot of Figure 6. Most of the capacity is installed in Western Europe with Germany as leading country. The mean PV power production, estimated with the IC and the capacity factors per country, amounts to 17.5 GW (153’300 GWh for the whole year 2019). The mean variability, which is the average change of PV power production when the weather regime shifts from one to another, amounts to 0.9 GW (1 GW is roughly the amount at which a nuclear power plant operates). This is about 5.1% of the total mean production. The maximum variability, which is the difference from the weather regime with the highest PV power production to the weather regime with the lowest PV power production per season, amounts to 3.0 GW. Which is a change in PV power production of 17.1%.

The planned total IC of the year 2030 is 386.5 GW (NECPs), which is about three times as much as in 2019. Most of the installed capacity is still located in Western Europe (Figure 6, second plot). The mean estimated PV power production increases to 52.3 GW. The mean and maximum variability also roughly triples compared to the year 2019 to 2.7 GW and 8.5 GW, respectively. Which is 5.2% and 16.3% of the mean PV power production. A details overview of the variability can be found in Figure 8 and Figure 9. Where the former shows the deviation (from the season mean) of PV power production per weather regime and season and the latter shows a consolidated (over all weather regimes) view per season.

3.2.1 Scenario 1 (S1) – PV power production and installed capacities from NECP 2030

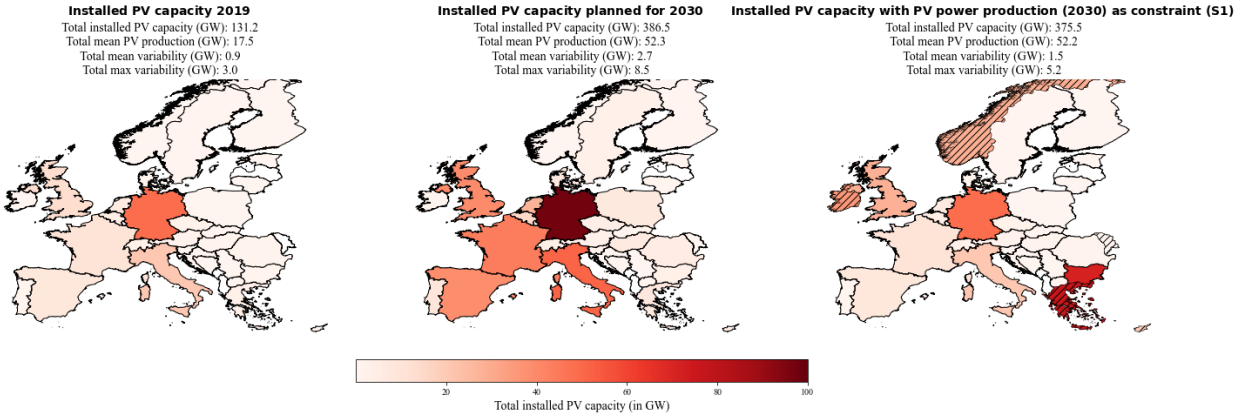

Figure 6: Current (2019), planned for the year 2030 (NECPs) and resulting from scenario 1 (S1) installed PV capacity distributions. S1 minimized the variability of PV power production with the constraint that the PV power production must be equal to the PV power production estimated for the year 2030 (NECPs). Hatched countries indicate that the upper bound (potential for roof-top mounted PV systems) is reached.

The IC distribution derived under the conditions of S1 is shown in third plot of Figure 6. The total mean PV power production is almost the same as the one estimated with NECPs for 2030 (0.1 GW difference), which was the constraint for this scenario. The mean variability could be reduced from 2.7 GW to 1.5 GW and the maximum variability could be reduced from 8.5 GW to 5.2 GW. This refers to a percentual reduction from 5.2% to 2.9% for the mean variability and from 16.3% to 10.0% for the maximum variability. The reduction of the variabilities, with keeping the PV power production constant, could be achieved with overall less total installed PV capacity of 375.5 GW (compared to 386.5 GW planned for 2030).

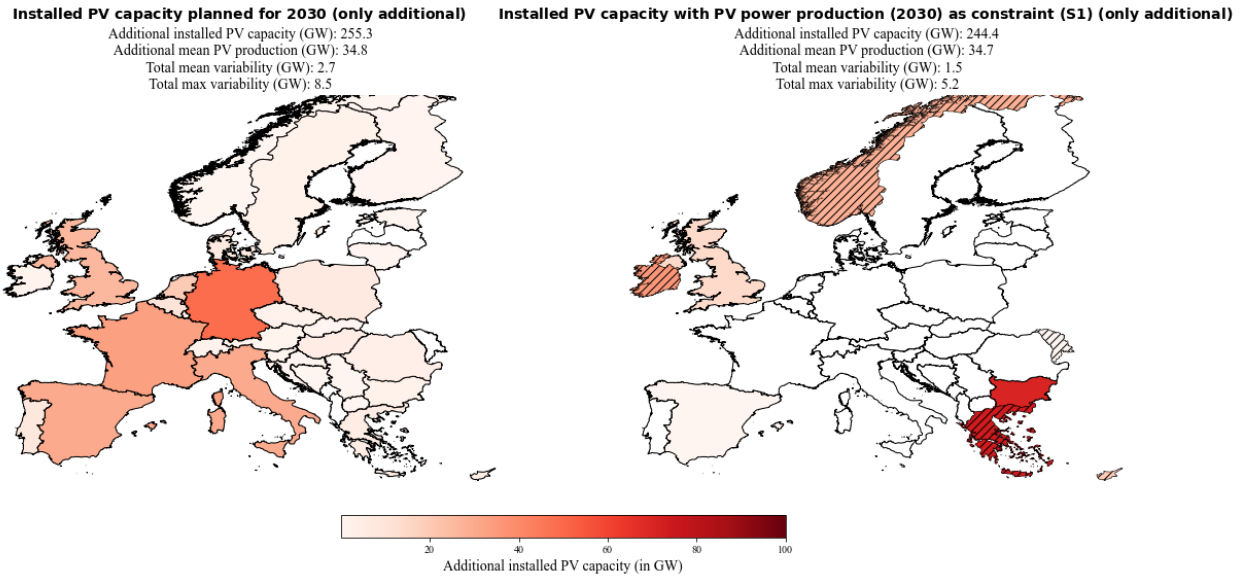

Figure 7: Additional installed PV capacities planned for the year 2030 (NECPs) and of scenario 1 (S1). S1 minimized the variability of PV power production with the constraint that the PV power production must be equal to the PV power production estimated for the year 2030 (NECPs). Hatched countries indicate that the upper bound (potential for roof-top mounted PV systems) is reached.

Figure 7 gives an overview where the additional installed PV capacity are distributed to. It shows the difference between the total installed PV capacity estimates for 2030 and the installed PV capacity from 2019 (which is also defined as the lower bound of the linear least-square problem). Our method chosen to reduce the variability clearly favours countries in South-eastern and North-western Europe. Hatched countries signalize that the installed capacity has reached the upper bound of the linear least-square problem, which is defined as the potential for roof-top mounted PV systems.

A detailed impression of the over- and underproduction for every weather regime and season compared to their seasonal mean is shown in Figure 8. The IC distribution for scenario one reduces the deviation of PV power production from the seasonal mean in 25 of 32 cases. It also shows that changes from under- to overproduction in weather regimes are possible with different distributions and vice versa.

The consolidate view of the variability (Figure 9) makes clear that the variability tends to be higher in mid-season (spring and autumn). Also, the maximum variability (black markers) is higher in mid-season with the peak in autumn for all three distributions. Figure 9 also shows that the distribution of S1 reduces the mean and maximum variability in in every season and in total.

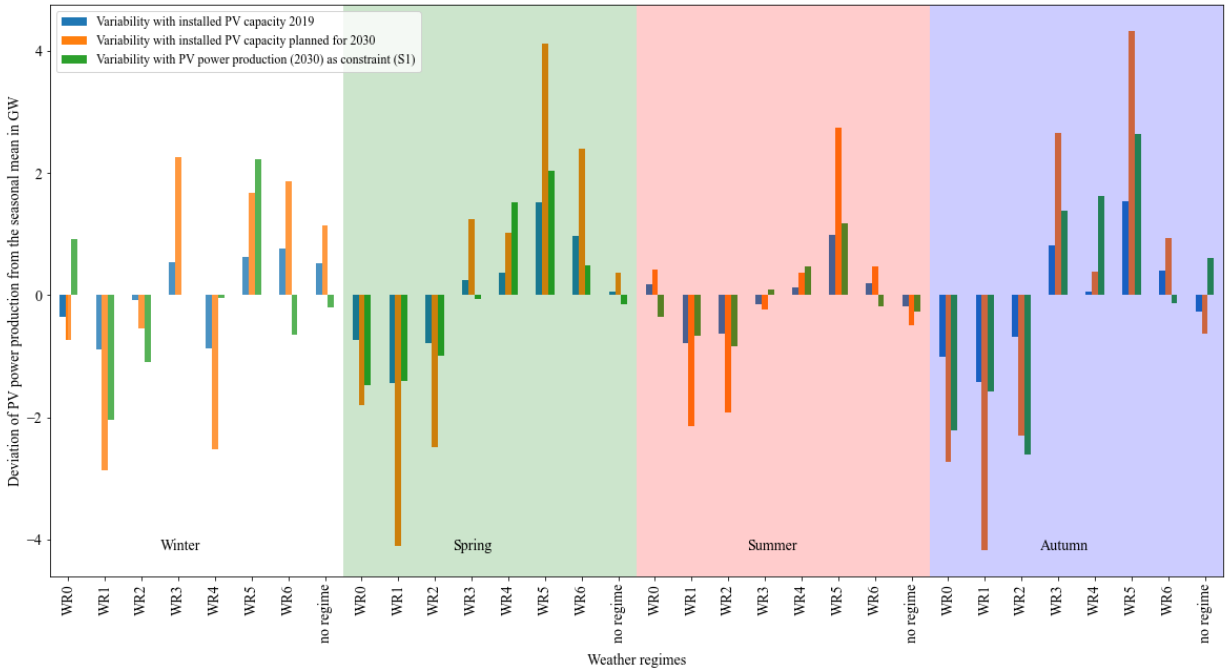

Figure 8: Deviation of the PV power production from the seasonal mean per weather regime and season. In blue the variability for the current situation (2019), in orange the estimated variability with the planned installed capacities for the year 2030 (NECPs) and in green the estimated variability with the installed capacity distribution for scenario 1.

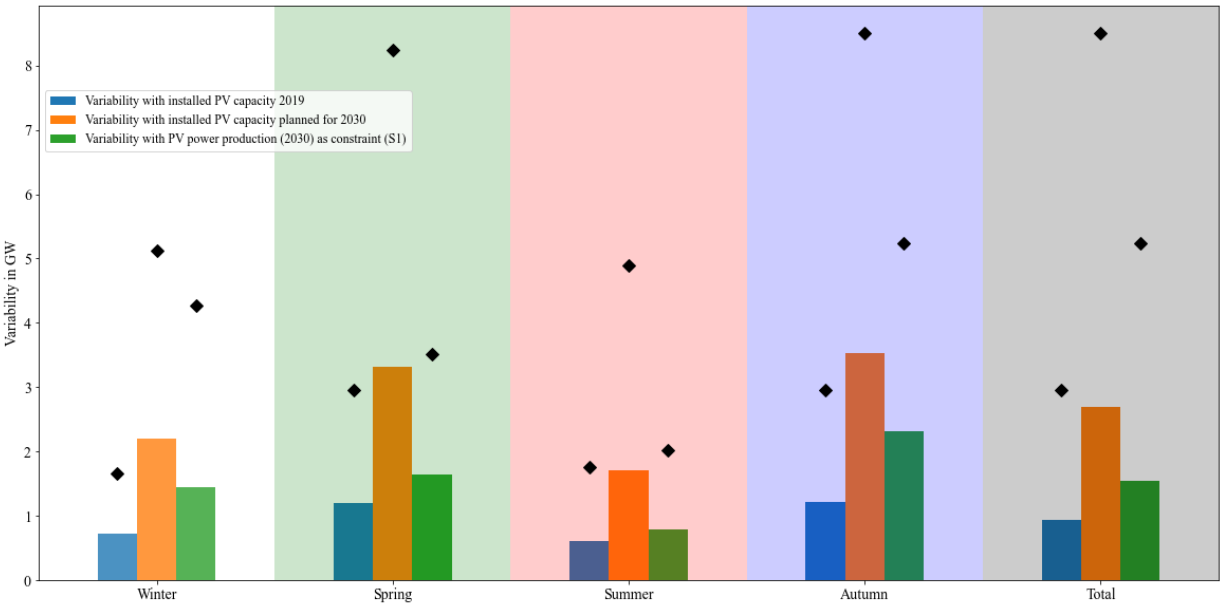

Figure 9: Mean (bars) and maximum (black markers) consolidated (over all weather regimes) variability per season and overall (total). In blue the variability for the current situation (2019), in orange the estimated variability with the planned installed capacities for the year 2030 (NECPs) and in green the estimated variability with the installed capacity distribution for scenario 1.

3.2.2 Scenario 2 (S2) – PV IC in 2050

The results of the three folded scenario two are shown in Figure 10. The top panel refers to the scenario calculated with the lowest estimate of 0.891 TW for the year 2050 by IRENA (S2-1), the second panel refers to the scenario calculated with the middle estimate of 1.94 TW for the year 2050 by Energy Watch Group(S2-2) and the third panel refers to the scenario calculated with the highest estimated of 8.8TW for the year 2050 by SolarPower Europe (S2-3). Since the latest estimate of 8.8TW is already higher than the sum of the potential IC for roof top mounted PV panels (which is used as upper bound), we defined the upper bound for this scenario five times large. The installed capacities per country are presented as percentage of the total installed capacity, to make comparison between the three results easier. The left side of each panel shows the interpolated installed PV capacity distribution to the year 2050. The interpolation is done so that the percentage of the total IC per country remains the same as in the year 2019. Which is way all three plots looks identical, but the total installed capacity and the variability is different.

The mean change in PV power production from one weather regime to another of the interpolation is 5.4% (remains for all interpolation the same because the percentual distribution remains as well). Our method was able to reduce it to 3.3%, 3.6% and 3.5% which refers to a reduction in mean variability of 2.5 GW, 4.7 GW and 22.1 GW, respectively. The maximum changes in PV power production from one weather regime to another of the interpolation is 16.9% (remains for all interpolations the same because the percentual distribution remains as well). This could be reduced to 10.7% (S2-1), 11.9% (S2-2) and 11.6% (S2-3) which refers to a reduction in maximum variability of 7.4 GW, 13.1 GW and 63.0 GW, respectively.

In the distributions of S2, South-eastern and North-western countries are still favoured (as in S1). But Spain and Italy also get a share of the capacities. Since the total installed capacities are much higher than in scenario one, the upper bounds of the countries are more often reached (hatched countries). The method reacts on that with placing the capacities to neighbouring. This can also be seen by a comparison of S2-1 (Figure 10, first row) and S2-2 (Figure 10, second row). With higher total installed capacities, the upper bounds are more often reached and mostly neighbouring countries receive the remaining capacities and the distribution gets flatter.

Since the upper bounds and the total installed capacity are both roughly five times higher in S2-3 (Figure 10, third row) than in S2-2 (Figure 10, second row), the distributions look very similar.

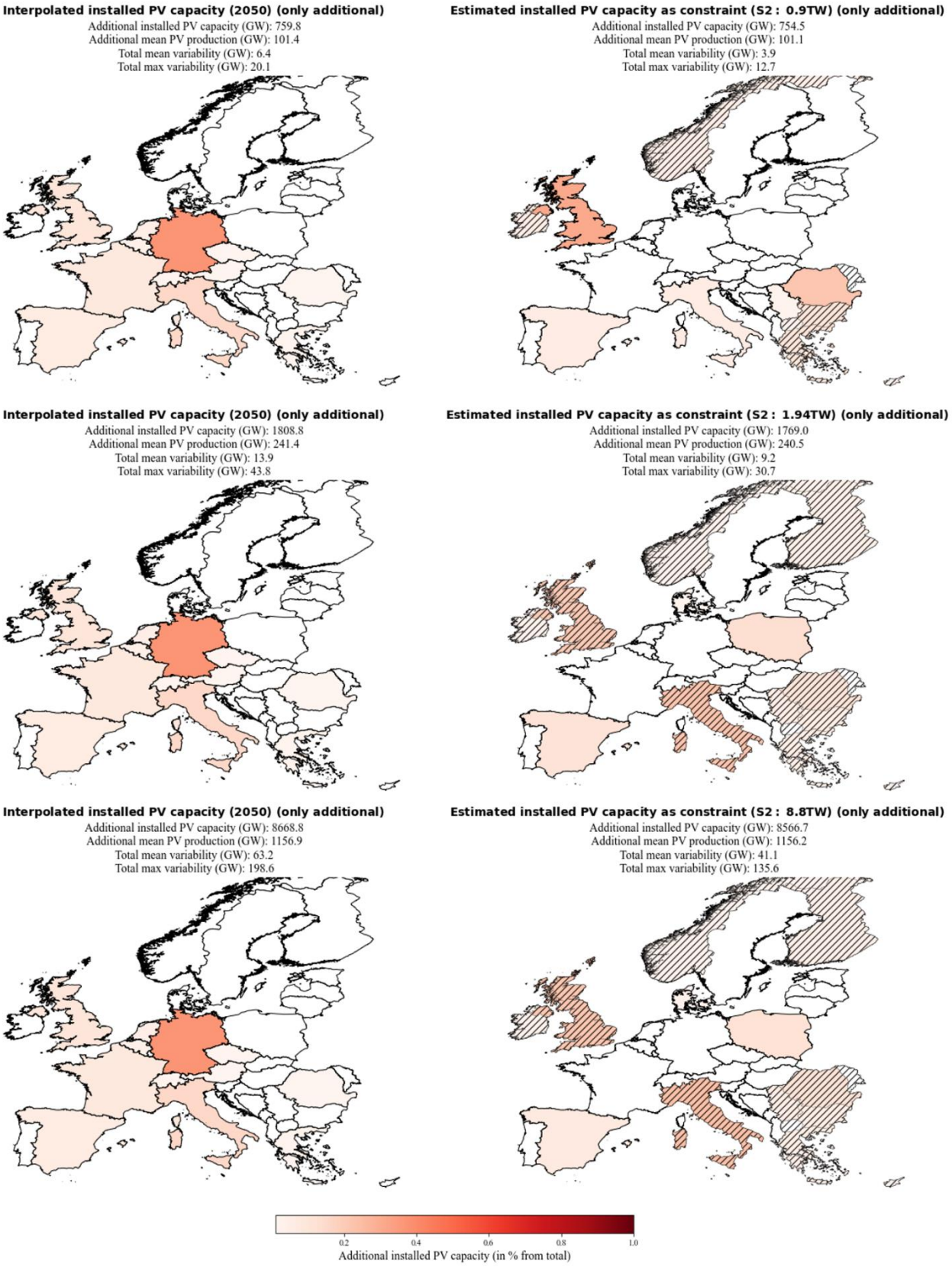

Figure 10: Additional installed PV capacities of 2050 (interpolated from the distribution of 2019) and of scenario 2-1, 2-2 and 2-3. Scenario 2-1, 2-2 and 2-3 minimize the variability of PV power production with the constraint that the power production must be equal to the PV power production estimated with the interpolations for the year 2050. Basis for the interpolation are the estimates by IRENA, Energy Watch Group and SolarPower Europe. Their estimated needed total installed PV capacity are 0.891 TW, 1.94TW and 8.8 TW for the year 2050. Hatched countries indicate that the upper bound (potential for roof-top mounted PV systems) is reached.

3.2.3 Scenario 3 (S3) – Cost minimization

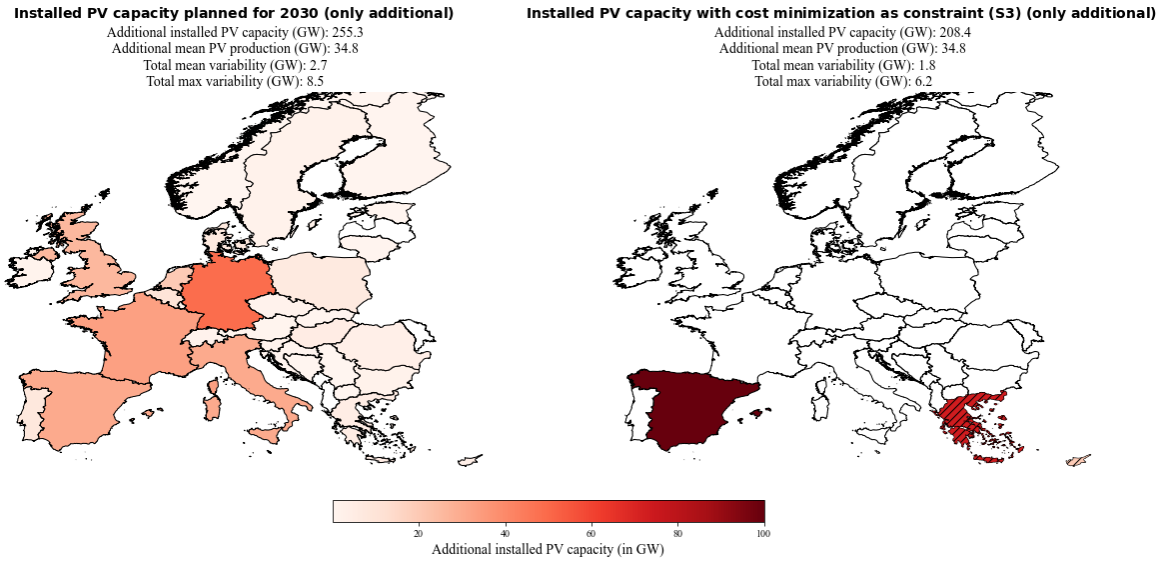

Figure 11: Additional installed PV capacities planned for the year 2030 (NECPs) and of scenario 3 (S3). S3 minimized the variability of PV power production and the installed PV capacities with the constraint that the power production must be equal to the power production estimated for the year 2030 (NECPs). Hatched countries indicate that the upper bound (potential for roof-top mounted PV systems) is reached.

With the focus on cost and variability minimization, we see a shift from the South-Eastern / North-western distribution (S1) to a South-eastern / South-western distribution (Figure 11, second plot). The mean variability could still be reduced from 2.7 GW to 1.8 GW (1.5 GW in S1). Which means that the mean variability reduction potential gets reduced from 44.4% (S1) to 33.3% (S3). The maximum variability could be reduced from 8.5 GW to 6.2 GW (5.2 GW in S1). Which decreases the reduction potential from 38.8% (S1) to 27.1%. The benefit of S3 is that it takes 35.9 GW less installed PV capacity to produce the same amount of electricity compared to S1.

By doing the same analysis with the estimate of 1.94TW for the year 2050 (Europe Watch Group, S2-2), we get the distribution shown in Figure 12. The method now places all the installed capacities to Southern countries. The mean variability gets reduced from 13.9 GW to 11.9 GW (9.2 GW in S2-2) and the maximum variability gets reduced from 43.8 GW to 35.0 GW (30.7 GW in S2-2). Which is a decrease of the mean variability reduction potential from 33.8% (S2-2) to 14.4% and a decrease of the maximum variability reduction potential from 29.9% to 20.1%. S3-2 needs 166.8 GW less installed capacity to produce on average 4.4 GW more electricity than S2-2.

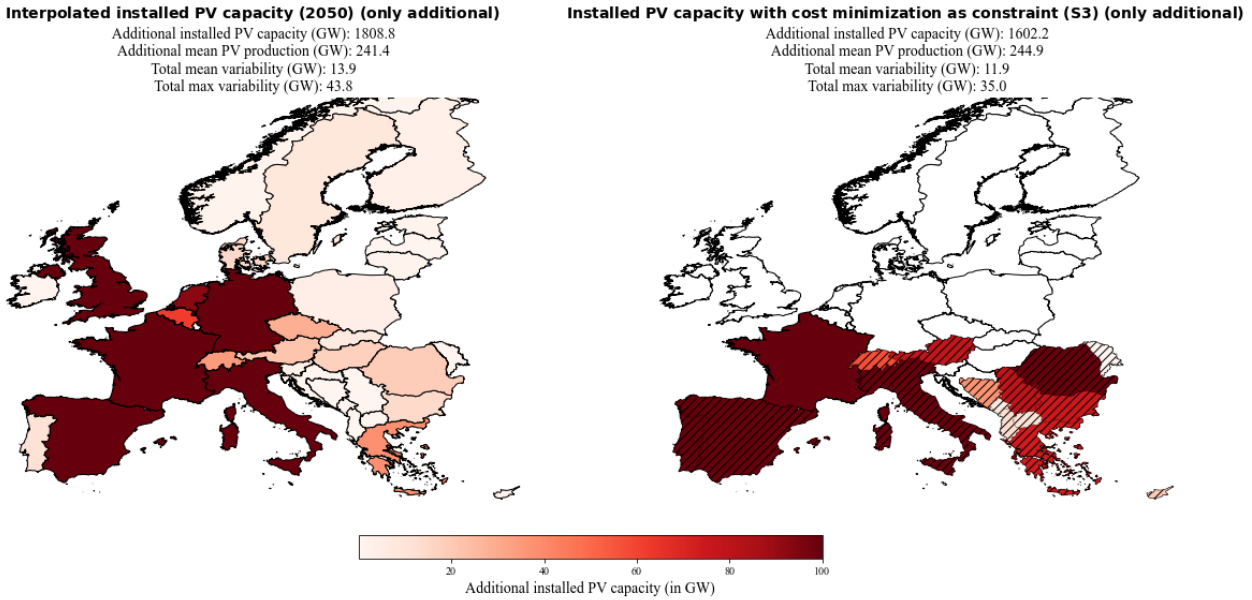

Figure 12: Additional installed PV capacities of 2050 (interpolated from the distribution of 2019 with the estimate of 1.94 TW installed PV capacity by the Energy Watch Group) and of scenario 3 (S3). S3 minimized the varability of PV power production and the installed PV capacities with the contraint that the power production must be equal to the power production estiamted for the year 2050. Hatched countries indicate that the upper bound (potential for roof-top mounted PV systems) is reached.

3.2.4 Scenario 4 (S4) –Coverage of country specific electricity consumption with PV systems

S4-1 enforces a flatter distribution because of the constraint that 10% of the country specific consumption must be produced with PV systems in the year 2030. 10% are chosen because already 13.5% of the sum of the latest available consumption data for each country equals the PV power production estimated for the year 2030 with the NECPs. And if we overshoot the total installed capacity from the NECPs a comparison would not be feasible.

The results are shown in Figure 13. All countries get their needed installed capacities to cover 10% of their consumption and the rest is again distributed to South-eastern and North-western Europe. The flatter distribution is at the expense of the variability reduction potential. It reduces from 44.4% (S1) to 29.6% for the mean variability and reduces from 38.8% to 29.4% for the maximum variability. Which means that we are reducing the total mean variability from 2.7 GW to 1.9 GW (1.5 GW in S1) and the total maximum variability from 8.5 GW to 6.0 GW (5.2GW in S1).

Interesting remark → with 13.5% → nearly same variability with bit more IC and same production

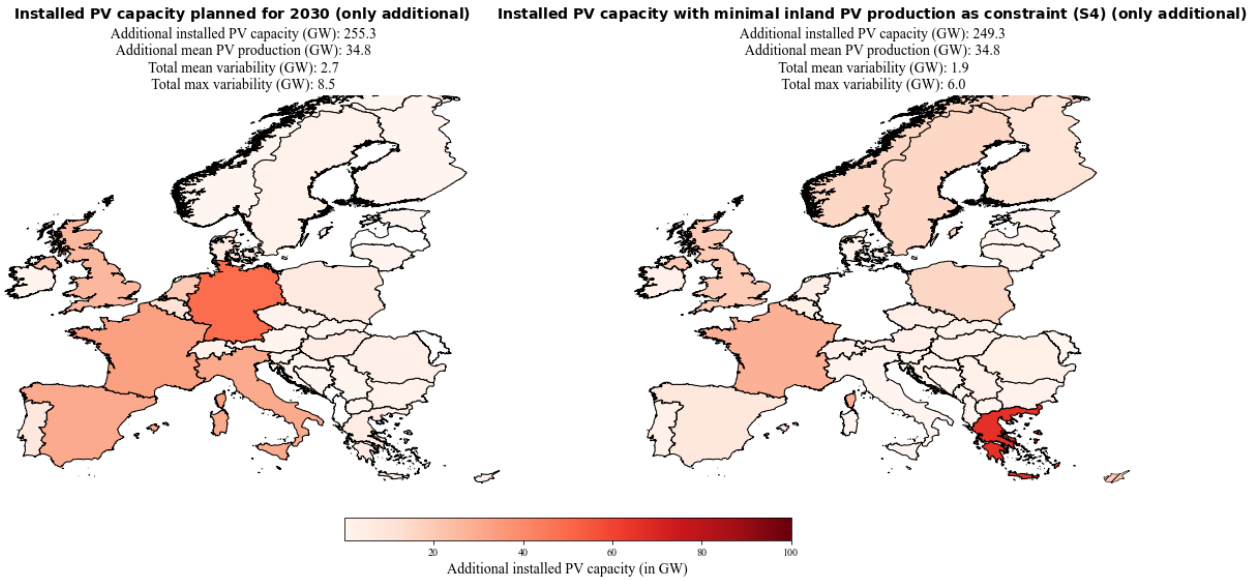

Figure 13 Additional installed PV capacities planned for the year 2030 (NECPs) and of scenario 4-1 (S4-1). S4-1 minimized the varability of PV power production with the contraint that the PV power production must be equal to the PV power production estiamted for the year 2030 (NECPs) and 10% of the inland electricity consumptions must be coverd with PV power production by the countries themselfe.

The same analyses but with the estimate of 1.94 TW installed capacity for the year 2050 by the Energy Watch Group and the constraint that 30% of the consumption per country must be covered with PV power production, yields to the results presented in Figure 14. The flatter distribution is again at the expense of the mean variability reduction potential. It decreases from 33.8% (S2-2) to 28.1%. Which is a reduction from 13.9 GW to 10.0 GW (9.2 GW in S2-2). Interestingly the maximum variability reduction potential increases within this scenario from 29.9% (S2-2) to 30.1%. Which is a reduction from 43.8 GW to 30.5 GW (30.7 GW in S2-2).

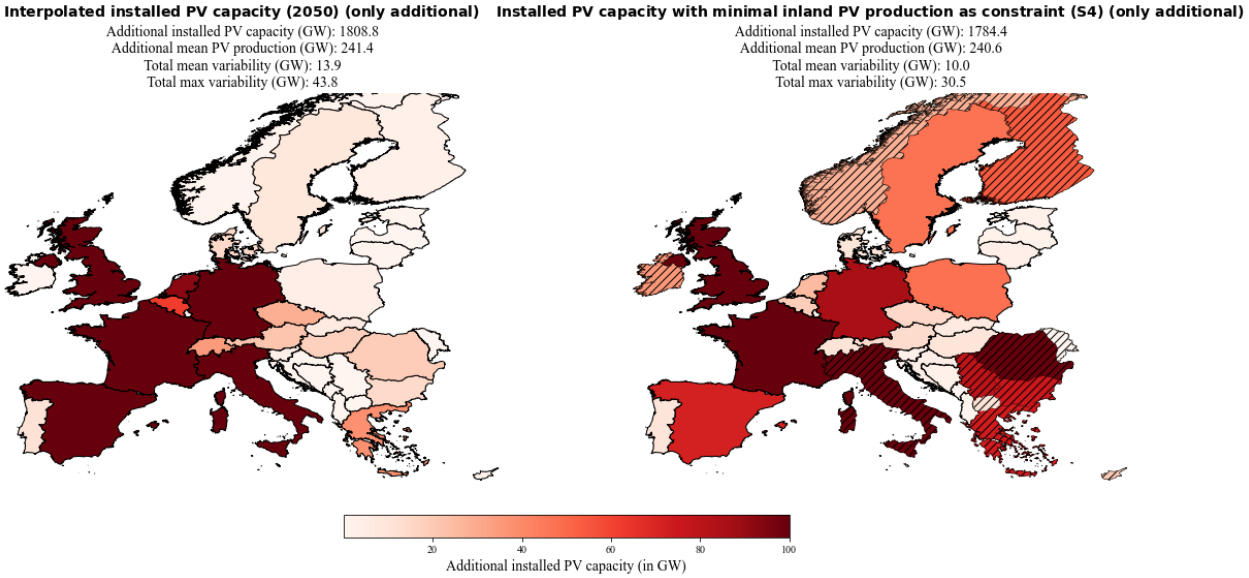

Figure 14: Additional installed PV capacities of 2050 (interpolated from the distribution of 2019 with the estimate of 1.94 TW installed PV capacity by the Energy Watch Group) and of scenario 4-1 (S4-1). S4-1 minimized the varability of PV power production with the contraint that the PV power production must be equal to the PV power production estiamted for the year 2050 and 30% of the inland electricity consumptions must be coverd with PV power production by the countries themselfe. Hatched countries indicate that the upper bound (potential for roof-top mounted PV systems) is reached.

An overview of all the important results of the various scenarios can be found in **Fehler! Verweisquelle konnte nicht gefunden werden.**. A detailed analysis of the over- and underproductions for every weather regime and season compared to their seasonal mean for all scenarios is shown in the appendix FIXXY – FIX XY. And the consolidate view of the variabilities for every scenario can also be found in the appendix FIXXY – FIXXY.

Table 3: Overview of all important variables of the various scenarios and their reference data.

	2019	2030 NECP	2050 1.94TW	S1	S2-1 0.891TW	S2-2 1.94TW	S2-3 8.8TW	S3-1 2030	S3-2 2050	S4-1 2030	S4-2 2050
Total Installed PV capacity [GW]	131.2	386.5	1940.0	375.5	885.6	1900.2	8697.8	339.6	1733.4	380.4	1915.6
Total mean PV production [GW]	17.5	52.3	258.9	52.2	118.6	258.0	1173.7	52.3	262.4	52.3	258.1
Total mean variability [GW]	0.9	2.7	13.9	1.5	3.9	9.2	41.1	1.8	11.9	1.9	10.0
Total max variability [GW	3.0	8.5	43.8	5.2	12.7	30.7	135.6	6.2	35.0	6.0	30.5
Mean variability / PV production [%]	5.1%	5.2%	5.4%	2.9%	3.3%	3.6%	3.5%	3.4%	4.5%	3.6%	3.9%
Max variability / PV production [%]	17.1%	16.3%	16.9%	10.0%	10.7%	11.9%	11.6%	11.9%	13.3%	11.5%	11.8%
Mean variability reduction [GW]	-	-	-	1.2	2.5	4.7	22.1	0.9	2.0	0.8	3.9
Max variability reduction [GW]	-	-	-	3.3	7.4	13.1	63.0	2.3	8.8	2.5	13.3
Mean variability reduction [%]	-	-	-	44.4%	39.1%	33.8%	35.0%	33.3%	14.4%	29.6%	28.1%
Max variability reduction [%]	-	-	-	38.8%	36.8%	29.9%	31.7%	27.1%	20.1%	29.4%	30.4%

3.3 Notes

To meet the EU's energy and climate targets for 2030, EU Member States need to establish a 10-year integrated national energy and climate plan (NECP) for the period from 2021 to 2030. I

2030 data → IRENA → plus missing countries!!?? → CH, UK

CF pro land vergleichen --> Doris Ide --> wie viel PV brauche ich für gleiche proiduktion in zb sweden than greece

CF pro land vergleichen --> Doris Ide --> wie viel PV brauche ich für gleiche proiduktion in zb sweden than greece

→ disupted by Colantuono 2014 and francois 2016 → nachlesen! NOA and solar radiation

WR3 → According to Wiel et al the impact of the Atlantic ridge on 2m temperature and wind are close to normal and therefore have a small impact on the energy sector. Nevertheless, his results also showed that the surface solar radiation over the Iberian Peninsula is higher than on average and over north-eastern Europe the surface solar radiation is slightly reduced.

- Einzelne ländern nullen

4. Discussion

4.1 Weather regimes classification

Our findings suggest that weather regime classification in Europe can be used to assess PV power output variability and can be used to reduce the variability with an optimal PV IC distribution. Although our weather regime classification is year around, our defined seven weather regimes include the four weather regimes which are found by many studies that focused only wintertime weather regime classification (Cassou, 2008; Michelangeli et al., 1995; van der Wiel et al., 2019; Vautard, 1990). Namely the Positive phase of the North Atlantic Oscillation (WR0), negative phase of the North Atlantic Oscillation (WR2), Atlantic ridge (WR3) and the Scandinavian blocking (WR6). Their frequencies (FIGX and tableY) suggest that we are in line with these studies because they are the weather regimes that occur most often in winter expect the Scandinavian blocking. This might be explained by the fact that the European blocking belongs to the top four weather regime during wintertime in our analysis instead of the Scandinavian blocking. Since these two weather regimes are very similar, one might be at the expense of the other because we are splitting them into two separate weather regimes. A comparison with the seven weather regimes defined year around by GRAMS shows that they are mostly in line with our weather regime classification. The comparison turns out to be challenging because although GRAMS defined the year around, he presents the weather regime results only for wintertime. His results include also the four already discussed weather regimes (in his study with slightly different naming convention). But contrary to our frequencies during wintertime his frequencies does not determine them as the most frequent ones in winter. Additionally to those four weather regimes, he determined the three weather regimes Atlantic trough, European blocking and Scandinavian trough. The European blocking is in line with our findings. Whereas Scandinavian trough in his study is mostly comparable with the European trough in our study. But as the names states the cyclone in his study is located over Scandinavian and, in our study, over North-western Europe. Additionally, the meridional dipole is more pronounced in our results. The Atlantic trough fits well with GRAMS study. Although the positive geopotential height anomaly in Southern Europe in our study is more pronounced which might be explained because summertime is also included in our results. These differences and the differences in the frequencies might be explained because GRAMS results only show the weather regimes in winter and because the method chosen to classify the weather regimes are slightly different. Overall, the weather regimes definition is coherent and fits well to the studies by others.

4.2 Capacity factor anomalies and surface weather variables

The surface weather variables anomalies (solar radiation and 2m temperature) and in direct consequence the CFs anomalies are fitting well with other studies. Especially the four well studied weather regimes in wintertime agrees mostly with other research.

We have encountered a negative correlation between the **positive phase of the North Atlantic Oscillation (WR0)** and the surface solar radiation anomalies in Northern Europe (FIG). A positive correlation can be seen for Southern Europe. Consequently, the CF anomalies behave similar. The correlation between NOA+ and surface solar radiation is in agreement with the study by Pozo-Vazquez et al. (2011) although it is disputed by Colantuono et al., (2014). The encountered similar longitudinal dipole of the PV CFs anomalies can also be observed in the study by Grams et al. (2017). The changes throughout the seasons are similar as well. The study by Van Der Wiel et al. (2019), which only focus on wintertime, stated that the surface solar radiation is close to normal during the NOA+. But their results also show a slightly North-South gradient. And our results agree with that in the way that the discrepancy is less pronounced in winter than in other seasons.

The observed negative correlation between the **negative phase of the North Atlantic Oscillation (WR2)**, the surface solar radiation and the CFs anomalies in Northern Europe (negative correlation for Southern Europe) tends to be more accepted. Which is also true for the overall negative temperature anomaly in Europe. (Grams et al., 2017; Hurrell et al., 2003; Pozo-Vazquez et al., 2011; van der Wiel et al., 2019). This is also in line with studies that stated the during the NOA- precipitation and cloud cover is enhanced (Jerez et al., 2013). Van der Wiel et al. (2019) identified that the combination of low temperature and lower than average wind speed during the NOA- is at the risk that the demand of electricity increases the supply of electricity in Northern Europe. Since the surface solar radiation is enhanced during NOA- it might be a possibility to reduce that risk.

The enhanced surface solar radiation and capacity factor anomalies in South-western Europe during the **Atlantic ridge (WR3)** is in agreement with Grams et al. (2017) and van der Wiel et al. (2019). Although the temperature anomalies in winter found by van der Wiel et al. (2019) are less pronounced compared to our temperature anomalies defined year around. But the changes throughout the season of the CF anomalies are rather high which gives reason to assume that the surface weather variables also are. Our identified changes throughout the seasons are mostly in line with Grams et al. (2017).

The anticyclone over Scandinavian during the **Scandinavian blocking (WR6)** brings higher than normal surface solar radiation to Northern Europe. The enhanced surface solar radiation caused by descending air and therefore clear sky condition is line with the study Amajama (2016). The resulting higher than normal 2m temperature and CFs anomalies, which is relatively constant for all seasons, are also observed by Grams et al. (2017) and van der Wiel et al. (2019).

These observations also hold for the **European blocking (WR5)**. Generally we see enhanced surface solar radiation anomalies and therefore enhanced CF anomalies in Central Europe where the Anticyclone is located (in line with Amajama, (2016)). The seasonal change is more pronounced which is partly agrees with Grams et al. (2017). The change from slightly positive CFs anomalies in Southern Europe in winter to slightly negative values in summer fit to the observation by Grams et al. (2017). But they do

not fit for Northern countries. We found slightly negative CF anomalies in winter, but their results show strongly positive values. The reason for the difference is not clear yet. But it seems like the seasonal cycle has a strong influence during this weather regime in our study. Positive CF anomalies in winter are mostly pronounced in Southern Europe. But than a northward shift towards summer can be observed and again southward shift in autumn, which is in line with the seasonal cycle of surface solar radiation. This obvious and strong influence of the seasonal cycle cannot be observed in the other weather regime and their CF anomalies.

The surface solar radiation and CF anomalies of the **European through (WR1)** do agree to an large extend with the Scandinavian through defined by Grams et al. (2017). Also, the changes throughout the season matches well. Main differences arise from Southern countries which tend to be more negative within our study in wintertime. This could be explained with the position of the cyclone which in our results are located more to the South. A comparison with study by Jones et al. (2020), who investigated in the impact of 29 Grosswetterlagen on the European Energy Sector, show that the PV power production anomalies of the Grosswetterlage TRW (trough Western Europe) and TM (through Central Europe), which are mostly comparable with the European through from our analyses, are more in line with our results.

The **Atlantic trough (WR4)** is the weather regime which agrees worst with the weather regimes defined by Grams et al. (2017). Mainly because of the positive geopotential height anomaly in Southern Europe which in our results are more pronounced. Therefore, it could be expected that the CFs anomalies and weather variables also do not fit well. Indeed the surface solar radiation and the CF anomalies in South-eastern Europe are higher than normal within our study contrary to Grams et al. (2017). Interestingly the negative surface solar radiation anomalies by Grams et al. (2017) in winter for Northern countries fit with our surface solar radiation anomalies for the whole year. But a look at the solar PV power output anomalies for Northern countries in winter in their study counterintuitive suggest positive values. Whereas our results suggest negative CF anomalies. This is more in line with the study by Jones et al. (2020) who also suggest negative solar power production anomalies in Northern Europe during the Grosswetterlagen SWZ (cyclonic South-westerly) and SWA (anticyclonic South-westerly), which are relatable to the Atlantic trough.

Solar radiance and 2m temperature

- NOA+ → Pozo Vasquez negative vorrleation → disupte by colantuono an francios
- NOA- → enhanced precipitation and cloud ccover er Curtis 2016
- Scnadinavian blocking → higher ssrd but cooler temp? amajama 2016
- Atlantic ridge → weakest relation to weather variables → barrier 2014 and van der wiel
- European trough → 2m temp Bloomfield 2020

4.3 Variability

Since the installed capacities of PV is still relatively small compared to the installed capacity of wind turbines, there are not many studies that focus on its variability. Therefore, we mainly compare our results with the study by Grams et al. (2017) who analysed its current variability but refuses to further investigate in its reduction potential for the same reason. An overview of the direct comparison between our and GRAMS results can be found in TABLEXY. They are presented in such a way that the difference in the total installed PV capacity is considered (131.2GW vs. 87.91GW).

	Winter	Spring	Summer	Autumn
PV power production / PV installed capacity 2019	6.6%	16.5%	19.6%	10.7%
PV power production / PV installed capacity Grams et al. (2017)	6.8%	16.7%	19.7%	10.9%
Maximum variability / PV power production 2019	19.3%	13.6%	6.8%	21.1%
Maximum variability / PV power production Grams et al. (2017)	31.8%	17.7%	5.1%	23.8%

The PV power production divided by the PV installed capacity are nearly identical. Which could be expected since the data source for the CF are the same and the percentual distribution of installed capacities from 2015 to 2019 in Europe did not change dramatically. Although the change was percentual distribution has not changed much it might explain the small differences in the results.

Contrariwise, the differences in the variability divided by the seasonal PV power production does not fit as well. The pattern from spring, to summer, to autumn seems to be alike and generally of similar sizes. But the results for winter show greater differences. Since PV power production is lowest in winter anyhow, and therefore also the absolute variability, it might play a less important role for general variability optimization considerations.

for the current variability fit well with the estimates by Grams et al. (2017).

2030 PV → 8.5GW / 2030 Wind 51.7 GW / 2015 wind 22.4 GW
2050 PV → 20.1-198.6GW

Current situation max var .3 GW 17.1% spring → GRAMS 2.6 GW spring (18%)
Mean production

	Winter	Spring	Summer	Autumn
Mean PV power production (2019)	8.6	21.7	25.7	14
Mean PV power production (GRAMS)	6.01	14.65	17.34	9.6

Max PV power production anomaly → always WR5 (EuBl) expect winter WR6 (ScBl) → GRAMS always EuBl (+1GW) expect summer

Min Prod always WR1 European through → GRAMS AT

	Winter	Spring	Summer	Autumn
WR0 (NOA+) / ZO	- / +	-- / -	+ / +	-- / --
WR1 (EUTr) / ScTr	-- / -	-- / --	-- / -	-- / -
WR2 (NOA-) / GL	- / -	-- / +	- / -	- / --
WR3 (AR) / AR	+ / +	+ / -	- / -	++ / -
WR4 (AT) / AT	-- / -	+ / --	+ /-	+ / --
WR5 (EuBl)	++ / ++	++ / ++	++ / +	++ / ++
WR6 (ScBl)	++ / +	++ / ++	+ / +	+ / +

5. Conclusion

In the present work, we could successfully assess the relation between weather regimes and PV power output variability.

Bremen 2010

- At themoment, it is not clear if transmission or storage is economically more advantageous
- Consequently, less energy from storage facilities is required to meet imbalances In case the consumption is higher than the current generation, either stored energy must be released or additional generation units must be activated. The activation of additional generation units requires that several units are operated in stand-by or in part-load. Both options are not economical for large fossil powered generation units. Nuclear power plants can not be used as they require lead times for scheduling up to 1 day. The power of small-scale gaspowered units can be increased very quickly, thus they are ideal to fulfil this kind of service. They run either with natural gas or gas from (renewable) biomass plants.

And in line with that the seasonal frequency (FIG XY) of theses weather regimes shows us that they occur more in winter than in the other seasons (nicht 100% NOAs schon aber andere nicht so).

Weather regime 1 and 4 are more difficult to assign wo well known weather regime.. But the low pressure field located a bit more southwar over the western coast of Europe. Weather regime 4 is most likely comparable with the Atlantic through. But one can clearly identify an high pressure filed in the Southern par of Europe which would be more typical fo a blocking situation. Finally, weather regime 5 is the European blocking situation which is often associated with warmen than seasonal average temperature over central Europe

Weather regime 5 is characterized by a blocking high pressure field like weather regime 5.

6. Appendix

	Winter (DJF)	Spring (MAM)	Summer (JJA)	Autumn (SON)
WR0	19.4%	13.7%	12.6%	12.4%
WR1	11.9%	16.0%	14.5%	16.4%
WR2	13.9%	10.1%	6.2%	9.1%
WR3	13.9%	12.5%	15.6%	16.6%
WR4	9.7%	14.3%	17.6%	11.7%
WR5	14.0%	13.3%	14.1%	12.6%
WR6	11.4%	13.1%	11.8%	14.1%
no regime	5.8%	7.0%	7.5%	7.0%

		PV power production anomaly 2019 (GW)
Winter Mean production: 8.6 GW	**WR0**	-0.36
	WR1	-0.89
	WR2	-0.08
	WR3	0.55
	WR4	-0.87
	WR5	0.62
	WR6	0.77
	no regime	0.52
Spring Mean production: 8.6 GW	**WR0**	-0.74
	WR1	-1.43
	WR2	-0.78
	WR3	0.25
	WR4	0.36
	WR5	1.53
	WR6	0.97
	no regime	0.05
Summer Mean production: 25.7 GW	**WR0**	0.18
	WR1	-0.78
	WR2	-0.63
	WR3	-0.16
	WR4	0.13
	WR5	0.98
	WR6	0.19
	no regime	-0.18
Autumn Mean production: 14.0 GW	**WR0**	-1.00
	WR1	-1.41
	WR2	-0.68
	WR3	0.82
	WR4	0.06
	WR5	1.54
	WR6	0.41
	no regime	-0.28

		PV power production anomaly 2019 (GW)	PV power production anomaly 2030 (GW)
Winter Mean production: 8.6 GW	**WR0**	-0.36	-0.74
	WR1	-0.89	-2.87
	WR2	-0.08	-0.55
	WR3	0.55	2.26
	WR4	-0.87	-2.52
	WR5	0.62	1.68
	WR6	0.77	1.87
	no regime	0.52	1.15
Spring Mean production: 21.7 GW	**WR0**	-0.74	-1.80
	WR1	-1.43	-4.11
	WR2	-0.78	-2.49
	WR3	0.25	1.24
	WR4	0.36	1.02
	WR5	1.53	4.12
	WR6	0.97	2.40
	no regime	0.05	0.36
Summer Mean production: 25.7 GW	**WR0**	0.18	0.42
	WR1	-0.78	-2.15
	WR2	-0.63	-1.92
	WR3	-0.16	-0.24
	WR4	0.13	0.36
	WR5	0.98	2.74
	WR6	0.19	0.47
	no regime	-0.18	-0.49
Autumn Mean production: 14.0 GW	**WR0**	-1.00	-2.72
	WR1	-1.41	-4.18
	WR2	-0.68	-2.30
	WR3	0.82	2.65
	WR4	0.06	0.39
	WR5	1.54	4.32
	WR6	0.41	0.93
	no regime	-0.28	-0.62

		PV power production anomaly 2019 (GW)
Winter **Mean production: 8.6 GW**	**WR0**	-0.36
	WR1	-0.89
	WR2	-0.08
	WR3	0.55
	WR4	-0.87
	WR5	0.62
	WR6	0.77
	no regime	0.52
Spring **Mean production: 21.7 GW**	**WR0**	-0.74
	WR1	-1.43
	WR2	-0.78
	WR3	0.25
	WR4	0.36
	WR5	1.53
	WR6	0.97
	no regime	0.05
Summer **Mean production: 25.7 GW**	**WR0**	0.18
	WR1	-0.78
	WR2	-0.63
	WR3	-0.16
	WR4	0.13
	WR5	0.98
	WR6	0.19
	no regime	-0.18
Autumn **Mean production: 14.0 GW**	**WR0**	-1.00
	WR1	-1.41
	WR2	-0.68
	WR3	0.82
	WR4	0.06
	WR5	1.54
	WR6	0.41
	no regime	-0.28

8. References

Amajama, J. (2016). Effect of Air Pressure on the Output of Photovoltaic Panel and Solar Illuminance (or Intensity). *International Journal of Scientific Engineering and Applied Science*, *2*(8), 139–144.

Branch, M. A., Coleman, T. F., & Li, Y. (1999). Subspace, interior, and conjugate gradient method for large-scale bound-constrained minimization problems. *SIAM Journal of Scientific Computing*, *21*(1), 1–23. https://doi.org/10.1137/S1064827595289108

Cassou, C. (2008). Intraseasonal interaction between the Madden-Julian Oscillation and the North Atlantic Oscillation. *Nature*, *455*(7212), 523–527. https://doi.org/10.1038/nature07286

Colantuono, G., Wang, Y., Hanna, E., & Erdélyi, R. (2014). Signature of the North Atlantic Oscillation on British solar radiation availability and PV potential: The winter zonal seesaw. *Solar Energy*, *107*, 210–219. https://doi.org/10.1016/j.solener.2014.05.045

Dawson, A. (2016). eofs: A Library for EOF Analysis of Meteorological, Oceanographic, and Climate Data. *Journal of Open Research Software*, *4*, 4–7. https://doi.org/10.5334/jors.122

Delucchi, M. A., & Jacobson, M. Z. (2011). Providing all global energy with wind, water, and solar power, Part II: Reliability, system and transmission costs, and policies. *Energy Policy*, *39*(3), 1170–1190. https://doi.org/10.1016/j.enpol.2010.11.045

Graabak, I., & Korpås, M. (2016). Variability Characteristics of European Wind and Solar Power Resources—A Review. *Energies*, *9*(6), 1–31. https://doi.org/10.3390/en9060449

Grams, C. M., Beerli, R., Pfenninger, S., Staffell, I., & Wernli, H. (2017). Balancing Europe's wind-power output through spatial deployment informed by weather regimes. *Nature Climate Change*, *7*(8), 557–562. https://doi.org/10.1038/nclimate3338

Heide, D., von Bremen, L., Greiner, M., Hoffmann, C., Speckmann, M., & Bofinger, S. (2010). Seasonal optimal mix of wind and solar power in a future, highly renewable Europe. *Renewable Energy*, *35*(11), 2483–2489. https://doi.org/10.1016/j.renene.2010.03.012

Hennermann, K., & Yang, X. (2018). *ERA5 data documentation*. European Centre for Medium-Range Weather Forecasts. https://confluence.ecmwf.int/display/CKB/ERA5+data+documentation

Hersbach, H., Bell, B., Berrisford, P., Biavati, G., Horányi, A., Muñoz Sabater, J., Nicolas, J., Peubey, C., Radu, R., Rozum, I., Schepers, D., Simmons, A., Soci, C., Dee, D., & Thépaut, J.-N. (2018). *ERA5 hourly data on pressure levels from 1979 to present.* Copernicus Climate Change Service (C3S) Climate Data Store (CDS). https://doi.org/10.24381/cds.bd0915c6

Huld, T., Gottschalg, R., Beyer, H. G., & Topič, M. (2010). Mapping the performance of PV modules, effects of module type and data averaging. *Solar Energy*, *84*(2), 324–338. https://doi.org/10.1016/j.solener.2009.12.002

Hulme, M. (2016). 1.5 °C and climate research after the Paris Agreement. *Nature Climate Change*, *6*(3), 222–224. https://doi.org/10.1038/nclimate2939

Hurrell, J. W., Kushnir, Y., Ottersen, G., & Visbeck, M. (2003). An overview of the north atlantic oscillation. *Geophysical Monograph Series*, *134*, 1–35. https://doi.org/10.1029/134GM01

IRENA. (2020a). Global Renewables Outlook: Energy transformation 2050. In *International Renewable Energy Agency*. https://www.irena.org/publications/2020/Apr/Global-Renewables-Outlook-2020

IRENA. (2020b). *Renewable capacity statistics 2020 International Renewable Energy Agency (IRENA)*.

Jäger-Waldau, A. (2019). PV Status Report 2019. In *EUR 29938 EN, Publications Office of the European Union*. https://doi.org/10.2760/326629

Jerez, S., Trigo, R. M., Vicente-Serrano, S. M., Pozo-VáZquez, D., Lorente-Plazas, R., Lorenzo-Lacruz, J., Santos-Alamillos, F., & MontáVez, J. P. (2013). The impact of the north atlantic oscillation on renewable energy resources in Southwestern Europe. *Journal of Applied Meteorology and Climatology*, *52*(10), 2204–2225. https://doi.org/10.1175/JAMC-D-12-0257.1

Jones, S., Lee, S. R., & Bloomfield, H. (2020). *Wintertime Impacts of Synoptic-Scale Weather Patterns on the European Energy Sector* (Issue August). University of Reading.

Lauret, P., Boland, J., & Ridley, B. (2013). Bayesian statistical analysis applied to solar radiation modelling. *Renewable Energy*, *49*, 124–127. https://doi.org/10.1016/j.renene.2012.01.049

Michelangeli, P. A., Vautard, R., & Legras, B. (1995). Weather regimes: recurrence and quasi stationarity. In *Journal of the Atmospheric Sciences* (Vol. 52, Issue 8, pp. 1237–1256). https://doi.org/10.1175/1520-0469(1995)052<1237:WRRAQS>2.0.CO;2

Mills, A., & Wiser, R. (2010). Implications of Wide-Area Geographic Diversity for Short- Term Variability of Solar Power. In *Energy*. https://doi.org/10.2172/986925

Muñoz Sabater, J. (2019). *ERA5-Land hourly data from 1981 to present.* Copernicus Climate Change Service (C3S) Climate Data Store (CDS). https://doi.org/10.24381/cds.e2161bac

Pedregosa, F., Varoquaux, G., Gramfort, A., Michel, V., Thirion, B., Grisel, O., Blondel, M., Prettenhofer, P., Weiss, R., Dubourg, V., Vanderplas, J., Passos, A., Cournapeau, D., Brucher, M., Perrot, M., & Duchesnay, E. (2011). Scikit-learn: Machine Learning in {P}ython. *Journal of Machine Learning Research*, *12*, 2825–2830.

Pfenninger, S., & Staffell, I. (2016). Long-term patterns of European PV output using 30 years of validated hourly reanalysis and satellite data. *Energy*, *114*, 1251–1265. https://doi.org/10.1016/j.energy.2016.08.060

Pozo-Vazquez, D., Santos-Alamillos, F. J., Lara-Fanego, V., Ruiz-Arias, J. A., & Tovar-Pescador, J. (2011). Hydrological, Socioeconomic and Ecological Impacts of the North Atlantic Oscillation in the Mediterranean Region. In *Hydrological, Socioeconomic and Ecological Impacts of the North Atlantic Oscillation in the Mediterranean Region* (Vol. 46, Issue December 2015). https://doi.org/10.1007/978-94-007-1372-7

Pozo-Vázquez, D., Tovar-Pescador, J., Gámiz-Fortis, S. R., Esteban-Parra, M. J., & Castro-Díez, Y. (2004). NAO and solar radiation variability in the European North Atlantic region. *Geophysical Research Letters*, *31*(5), n/a-n/a. https://doi.org/10.1029/2003gl018502

Ram, M., Bogdanov, D., Aghahosseini, A., Oyewo, A., Gulagi, A., Child, M., & Fell, H.-J. (2019). Global Energy System based on 100% Renewable Energy – Power, Heat, Transport and Desalination Sectors. *Study by Lappeenranta University of Technology and Energy Watch Group*, *1*(March), 1–321.

Ram, M., Bogdanov, D., Aghahosseini, A., Oyewo, S., Gulagi, A., Child, M., & Breyer, C. (2017). Global Energy System based on 100% Renewable Energy – Power Sector. *LUT Scientific and Expertise Publications : Raportit Ja Selvitykset - Reports*.

Ridley, B., Boland, J., & Lauret, P. (2010). Modelling of diffuse solar fraction with multiple predictors. *Renewable Energy*, *35*(2), 478–483. https://doi.org/10.1016/j.renene.2009.07.018

Rogers, J. C. (1997). North Atlantic storm track variability and its association to the North Atlantic oscillation and climate variability of Northern Europe. *Journal of Climate*, *10*(7), 1635–1647. https://doi.org/10.1175/1520-0442(1997)010<1635:NASTVA>2.0.CO;2

Santos-Alamillos, F. J., Pozo-Vázquez, D., Ruiz-Arias, J. A., Von Bremen, L., & Tovar-Pescador, J. (2015). Combining wind farms with concentrating solar plants to provide stable renewable power. *Renewable Energy*, *76*(2015), 539–550. https://doi.org/10.1016/j.renene.2014.11.055

SolarPower Europe and LUT University. (2020). *100% Renewable Europe - How to make Europe's energy system climate-neutral before 2050*. 64.

Stram, B. N. (2016). Key challenges to expanding renewable energy. *Energy Policy*, *96*, 728–734. https://doi.org/10.1016/j.enpol.2016.05.034

Sweerts, B., Pfenninger, S., Yang, S., Folini, D., van der Zwaan, B., & Wild, M. (2019). Estimation of losses in solar energy production from air pollution in China since 1960 using surface radiation data. *Nature Energy*, *4*(8), 657–663. https://doi.org/10.1038/s41560-019-0412-4

van der Wiel, K., Bloomfield, H. C., Lee, R. W., Stoop, L. P., Blackport, R., Screen, J. A., & Selten, F. M. (2019). The influence of weather regimes on European renewable energy production and demand. *Environmental Research Letters*, *14*(9), 094010. https://doi.org/10.1088/1748-9326/ab38d3

Vautard, R. (1990). Multiple weather regimes over the North Atlantic: analysis of precursors and successors. *Monthly Weather Review*, *118*(10). https://doi.org/10.1175/1520-0493(1990)118<2056:MWROTN>2.0.CO;2

Wallace, J. M., & Hobbs, P. V. (2006). *Atmospheric Science: An Introductory Survey* (2nd ed.). Amsterdam ; Boston : Elsevier Academic Press, [2006].

Wild, M., Folini, D., Henschel, F., Fischer, N., & Müller, B. (2015). Projections of long-term changes in solar radiation based on CMIP5 climate models and their influence on energy yields of photovoltaic systems. *Solar Energy*, *116*, 12–24. https://doi.org/10.1016/j.solener.2015.03.039

Comments/Notes

Solarpowereurope →

In 2050, solar PV alone has installed capacities between 4.7 TW in the Laggard scenario, 7.7 TW in the Moderate scenario and 8.8 TW in the Leadership scenario.

IRNEA

- Solar PV could cover a quarter of global electricity needs by mid-century, becoming the second largest generation source after wind.
- Global capacity must reach 18 times current levels, or more than 8 000 gigawatts by 2050.
- Asia would continue to dominate solar PV use, with over 50% of installed capacity, followed by North America (20%) and Europe (10%).
- 8000gigawatts*0.1 = 800gigawatts → in excel from IRENA 891

Large-scale integration of renewable energies and impact on storage demand in a European renewable power system of 2050

The results for the base scenario show a total installed generation capacity of 4,550 GW, which splits up into PV and WT in a ratio of 60:40 on global scale for the EUMENA regions. → 2730GW

Zappa

603-926GW je nach Szenario → Is a 100% renewable European power system feasible by 2050?

Ec.europe.eu

According to a recent 100% RES scenario of the Energy Watch Group, the EU needs to increase its PV capacity from 117 GW to over 630 GW by 2025 and 1.94 TW by 2050 in order to cover 100% of its electricity needs by renewable energy.

This is approximately half of the estimates (1.95TW) by Ram et al. (2017) whose study highlights the feasibility and the socio-economic viability of a transition to a 100% renewable electricity generation electricity system. → SCHNITT WIRD GEBRAUCHT???